Meson spectroscopy using mixed action setups with twisted mass sea quarks

Joshua Berlin

Master Thesis in Physics

Institute for Theoretical Physics
Johann-Wolfgang-Goethe-University, Frankfurt am Main

October 21, 2013

Supervisor: Prof. Dr. M. Wagner
Second advisor: Prof. Dr. O. Philipsen

Erklärung gemäß §28 (12) der Prüfungs- und Studienordnung (2011) des Bachelor und Masterstudiengang Physik der Johann Wolfgang Goethe-Universität.

Hiermit erkläre ich, dass ich die Arbeit selbständig und ohne Benutzung anderer als der angegeben Quellen und Hilfsmittel verfasst habe. Ferner erkläre ich, dass die Arbeit, auch nicht auszugsweise, für eine andere Prüfung oder Studienleistung verwendet worden ist.

Joshua Berlin

Abstract

This work investigates parity and isospin mixing effects of Wilson twisted mass quarks in mesonic spectral quantities. Based on gauge configurations with $N_f = 2+1+1$ flavors of twisted mass quarks, different valence actions are applied to reduce symmetry breaking effects. In total four different valence actions are chosen: Wilson and Wilson twisted mass quarks, with and without the clover term.
When considering such a mixed action approach, tuning of the valence and sea quark sector becomes of central importance. Demanding suitable matching conditions is mandatory for a consistent continuum limit, so that correct results are obtained.
Results for quantities as the pion, D meson and J/ψ are presented and discussed in all four action setups, at the end of the work.

Kurzfassung

In dieser Arbeit werden Paritäts- und Isospin-Mischungseffekte, für Wilson twisted mass Quarks, in ausgewählten Mesonen untersucht. Basierend auf Eichkonfigurationen mit $N_f = 2 + 1 + 1$ flavors von Wilson twisted mass Quarks, werden im Valenzsektor unterschiedliche Wirkung eingesetzt um jene Effekte zu reduzieren, die durch gebrochene Symmetrien auftreten. Insgesamt werden dazu vier verschiedene Valenzwirkungen untersucht: Wilson und Wilson twisted mass Quarks, mit und ohne Cloverterm.
Bei einer Methode wie einem solchen mixed action setup ist das Anpassen von Valenz- und See-Sektor von zentraler Wichtigkeit. Nur für präzise Übereinstimmungen beider Setups, ist das Kontinuum Limit wohl definiert und erlaubt korrekte Aussagen.
Zum Abschluss werden die Ergebnisse von Observablen wie dem Pion, D Meson und J/ψ, für alle untersuchten Wirkungen, präsentiert und diskutiert.

Contents

1 Introduction

The standard model is a non-abelian gauge theory with the symmetry group $SU(3) \times SU(2) \times U(1)$. Quantum chromodynamics (QCD) - the $SU(3)$ component - is a theory of the strong interaction between quarks and gluons, which is responsible for the formation of hadrons. Field theories in general are systems with an infinite number of degrees of freedom. To avoid divergent results a regularization of the theory by an *ultraviolet* cut-off is mandatory. For weak couplings - $SU(2)$ and $U(1)$ - the expansion of the path integral in the coupling constant leads to the well-known Feynman diagrams, which are then regularized order by order and allow precise results.
However, for strong couplings the growth of the coupling constant in the infrared requires a non-perturbative approach in order to investigate low energy properties. In 1974 K. Wilson [1] proposed lattice gauge theory as a regularization of QCD. In lattice QCD the euclidean space-time is discretized on a hypercubic lattice, with lattice spacing a. Quark fields are living on the lattice sites, and gauge fields on the links connecting sites. The lattice spacing a acts as the earlier demanded ultraviolet cut-off, rendering a finite quantum field theory. Continuum results are recovered by demanding an infinite number of lattice sites, and sending the lattice spacing to zero.

The foundation of this work is the lattice QCD formulation with so-called *twisted mass* fermions, an extension of the original proposed formulation by Wilson. Though it is a rather recent approach, by today it is already well established. With the original purpose to eliminate unphysical zero modes to gain a suitable (partially) quenched approximation, this formulation quickly turned out to be used much more extensive.
In 2001 Frezzotti and Rossi showed [2, 3], that scaling violations can be reduced to $\mathcal{O}(a^2)$ by a modification of the standard Wilson mass term of $m \longrightarrow m + i\mu\gamma_5\tau_3$ and tuning the theory to "maximal twist". In the continuum limit, a chiral rotation shows that this modification is equivalent to conventional QCD. This property is often referred to as "automatic $\mathcal{O}(a)$ improvement" and is a major advantage of the tmLQCD (twisted mass Lattice QCD) formulation. Further advantages are that the twisted mass term also acts as an infrared cutoff and simplifies mixing patterns in the renormalization procedure.
On the other hand, the major drawback of the twisted mass approach is an explicit breaking of parity and isospin symmetry at finite lattice spacing, only restored when the continuum limit is reached. Due to the automatic $\mathcal{O}(a)$ improvement this breaking is an $\mathcal{O}(a^2)$ effect, as simulations in a quenched approximation confirm [4, 5].

Hadron spectroscopy, adapting the Wilson twisted mass lattice discretization for the quark fields, is highly affected by these explicitly broken symmetries. Hadrons are classified by quantum numbers, in particular isospin I, angular momentum J and parity P. The study of a hadron thus requires a suitable creation operator O such that, acting on the vacuum $|\Omega\rangle$, $O|\Omega\rangle$ has the same quantum numbers $I(J^P)$ as the hadron of interest. In case of broken symmetries for the tmLQCD formulation, these quantum numbers are however only approximate quantum numbers, restored in the continuum.

In the calculation of hadrons with two different parity states or isospins of $I_z = 0$ with $I = 0$ or $I = 1$, a mixing pattern is always present. For a rigorous calculation of e.g. hadron masses from different parity sectors this pattern gives rise to two times the original needed correlation functions. This problem grows when considering several states with the motivation of investigating the overlap of different operators.

Computations with Wilson twisted mass fermions, tuned to maximal twist, have shown to yield precise results for pseudo scalar masses down to $m_{\mathrm{PS}} \approx 300$ MeV, i.e. with very low statistical fluctuations, e.g. for two mass-degenerate flavors of quarks [6]. This makes pseudo scalar meson masses ideal for scale setting, or tuning of masses, as it will be shown in section 3.2.
The study of scalar mesons is however, due to the mentioned broken parity symmetry, more difficult than pseudo scalar mesons using a Wilson twisted mass lattice discretization. Especially those states are a long term motivation of this work. The investigation of possible tetraquark candidates in the light scalar [e.g. $f_0(500)\, J^P = 0^+$, $K_0^*(800)\, J^P = 0^+$, $f_0(980)\, J^P = 0^+$, $a_0(980)\, J^P = 0^+$] and heavy scalar [e.g. $D_{s0}^*(2317)\, J^P = 0^+$, $D_{s1}(2460)\, J^P = 1^+$, or charmonium states X and Z] meson sector is of great current interest. A prominent example for this interest is probably found in the PANDA (anti-Proton ANnihilation at DArmstadt) program as part of FAIR (Facility for Accelerated Ion Research) in Darmstadt. There, (among others topics) the spectroscopy of the charmonium spectrum and D meson states are planned to be measured with an accuracy of about 100 keV above, or close to threshold.

Instead of the twisted mass action one could think of using different lattice discretizations to get rid of the disadvantage of an explicit broken parity and isospin symmetry, as for example, using standard Wilson fermions, where parity and isospin are exact symmetries. The major aspect of this work is indeed to investigate other action setups, different from Wilson twisted mass fermions, with the purpose of improving the spectroscopy of mesonic quantities. But, however, generating gauge field configurations is a HPC (High Performance Cluster) expensive task, so that an intermediate step is adopted here. Instead of generating gauge field configurations for all the action setups of interest, an approach of *mixed action setups* is chosen. In this setup, the action of interest is only employed in the valence quark sector, while in the sea quark sector gauge field configurations, with Wilson twisted mass discretization, are kept throughout the work.
It is then mandatory to relate the valence and the sea quark sector, such that the validity of the results is unharmed. This particular tuning process is rather time intensive compared to other computations and was mainly performed, by relating pseudo scalar masses.

In total four different lattice discretizations were investigated in this work. On one hand the unitary setup of Wilson twisted mass valence quarks on Wilson twisted mass sea quarks, functioning as a reference and tuning point. Further standard Wilson fermions were employed in the valence sector, realized by setting the twisted mass parameter to zero, i.e. $\mu = 0$. Finally an additional expansion of the actions, by adding the clover action to both of these valence actions, i.e. Wilson twisted mass + clover fermions and

Wilson + clover fermions, were considered.
The choice of Wilson fermions in the valence quark sector is of rather obvious nature, since, and this was already stated, parity and isospin are exact symmetries in this action setup, i.e. eliminating parity and isospin mixing completely. The drawback is that Wilson fermions by itself suffer from $\mathcal{O}(a)$ contributions, that can be numerically too large. By further application of the clover term to the action these $\mathcal{O}(a)$ contributions are assumed to be eliminated precisely (a more detailed explanation will follow). As a $\mathcal{O}(a)$ improved theory, with parity and isospin as exact symmetries, this action setup was expected to be of comparable quality as the unitary setup, with twisted mass valence quarks on twisted mass sea quarks.
In the last of the investigated mixed action setups, the clover term is added to the twisted mass valence action. This approach however, may at first appear strange, considering that the clover term in terms of the Symanzik improvement procedure was designed to remove $\mathcal{O}(a)$ contributions from the standard Wilson action. It is expected [7], that the effect of the clover term on the, already $\mathcal{O}(a)$ improved, Wilson twisted mass discretization could lead to a further reduction of the remaining $\mathcal{O}(a^2)$ contributions. With the twisted mass formulation as a discretization that only suffers from $\mathcal{O}(a^{2n})$ contributions in physical observables, such a reduction would be of great value in particular, but also for ongoing hadron spectroscopy projects like [8, 9, 10].

Parts of this work have been presented on the 31$^{\text{st}}$ International Symposium on Lattice Field Theory and were published [11].

1.1 Outline

In this thesis mixed action approaches with twisted mass sea quarks are investigated, with respect to their impact on parity and isospin mixing contributions as well as their application for spectroscopy.
In the following a brief outline of the sections in this work, including their particular purposes will be given.

After this introductory section the theoretical background, relevant for this thesis, will be summarized. A detailed discussion of technical aspects is not intended. However the basic principles of Wilson twisted mass are introduced and the most important quantities will be presented. The following part covers further aspects, like the extraction of meson masses on the lattice.
Section three presents the numerical results produced in this work. The tuning process, necessary for consistent results within all four setups is explained such as the setups in more detail. Right after computed mesonic quantities, like effective masses are presented and commented. Isospin breaking effects are briefly considered. In the last section a summary of results of this thesis is given with an additional conclusion of the results obtained.

1.2 Notation

Throughout this work mostly a compact notation was chosen, where indices are dropped in order to make the reading more convenient. However, for a better understanding indices are brought up sometimes during this work to highlight some details. The structure for a fermion field is then

$$\chi_A^{a,(m)}. \tag{1.1}$$

Lower case letters in the upper indices denote color indices, capital letters in the lower indices denote spin indices. Flavor indices are also denoted by lower case letters in the upper indices, but with an additional bracket.

Additional to the spatial L and temporal T extension of the lattice, the overall lattice volume will be denoted $L^3 \times T = \Lambda$ and the spatial volume $L^3 = \Lambda_3$.

The Pauli matrices are

$$\tau_1 = \begin{pmatrix} 0 & 1 \\ 1 & 0 \end{pmatrix}, \quad \tau_2 = \begin{pmatrix} 0 & -i \\ i & 0 \end{pmatrix}, \quad \tau_3 = \begin{pmatrix} 1 & 0 \\ 0 & -1 \end{pmatrix}. \tag{1.2}$$

Dirac matrices are used in the chiral representation

$$\gamma_0 = \begin{pmatrix} 0 & -1 \\ -1 & 0 \end{pmatrix}, \quad \gamma_j = \begin{pmatrix} 0 & -i\tau_j \\ i\tau_j & 0 \end{pmatrix}, \quad j \in \{1,2,3\}, \tag{1.3}$$

$$\gamma_5 = \gamma_0\gamma_1\gamma_2\gamma_3 = \begin{pmatrix} 1 & 0 \\ 0 & -1 \end{pmatrix}. \tag{1.4}$$

2 Theoretical Background

2.1 Basic principles

In this section an overview of those aspects of lattice QCD, relevant for this work, will be given. For a more detailed introduction into the topic cf. e.g. [12, 13, 14, 15, 16, 17, 18].

2.1.1 Standard Wilson fermion action

Introducing the well known lattice formulation of Wilson fermions

$$S_{\mathrm{F}}[\psi, \bar{\psi}, U] = a^4 \sum_{x \in \Lambda} \bar{\psi}(x) D_W(m) \psi(x), \tag{2.1}$$

with only one flavor for simplicity.

$$D_W(m) = \frac{1}{2} \left(\gamma_\mu \left(\nabla_\mu + \nabla_\mu^* \right) - a r \nabla_\mu \nabla_\mu^* \right) + m \tag{2.2}$$

denotes the standard *Wilson operator* and ∇_μ, ∇_μ^* are the gauge covariant forward and backward derivative. m is the *physical quark mass* and parameter r is the *Wilson parameter*, set to 1 hereafter.
The purpose of the *Wilson term* $-a\nabla_\mu\nabla_\mu^*$ is the removal of so-called *doublers*. Doublers are lattice artifacts that are found after performing a Fourier transformation of the lattice Dirac operator and occur as unwanted poles of the momentum space propagator in every corner of the Brillouin zone. The Wilson term is designed to cancel every unwanted pole in momentum space, except the momentum zero pole.

2.1.2 Wilson twisted mass lattice QCD

The Wilson twisted mass formulation of lattice QCD is a particular type of Wilson fermions, where a twisted mass term is added to the standard, unimproved Wilson-Dirac operator. For an introduction to the concept of the twisted mass discretization consider the standard Wilson action (2.1) in the continuum for $N_f = 2$ degenerate quarks

$$S_{\mathrm{F}}[\psi, \bar{\psi}, A] = \int \mathrm{d}^4x \; \bar{\psi}(x) \left(\gamma_\mu D_\mu + m \right) \psi(x). \tag{2.3}$$

Performing an axial rotation ω_1

$$\psi(x) = e^{\frac{i}{2}\omega_1 \gamma_5 \tau_3} \chi(x), \quad \bar{\psi}(x) = \bar{\chi}(x) \, e^{\frac{i}{2}\omega_1 \gamma_5 \tau_3}, \tag{2.4}$$

leaves the form of the action invariant, but transforms the mass term $m \longrightarrow m \, e^{i\omega_1 \gamma_5 \tau_3}$. With an additional isovector rotation ω_2

$$m_q + i\mu_q \gamma_5 \tau_3 = m \, e^{\frac{i}{2}\omega_2 \gamma_5 \tau_3}, \tag{2.5}$$

and demanding $\omega_1 = \omega_2$, the twisted mass QCD action is obtained

$$S_{\mathrm{F}}[\chi, \bar{\chi}, A] = \int \mathrm{d}^4x \; \bar{\chi}(x) \left(\gamma_\mu D_\mu + m_q + i\mu_q \gamma_5 \tau_3\right) \chi(x), \tag{2.6}$$

where m_q denotes the *untwisted quark mass* and μ_q the *twisted mass*. In the continuum both formulations are equivalent, however, at finite lattice spacing this is not the case due to an explicit breaking of axial symmetry by the Wilson term

$$S_{\mathrm{F}}[\chi, \bar{\chi}, U] = a^4 \sum_x \bar{\chi}(x) \left(D_W(m_0) + i\mu_q \gamma_5 \tau_3\right) \chi(x). \tag{2.7}$$

Making Wilson and Wilson twisted mass two different lattice regularizations.
For the discretized Wilson twisted mass action m_0 is referred to as the *bare untwisted quark mass*. Fermion fields were presented in the *physical basis* $\{\psi, \bar{\psi}\}$ and the *twisted basis* $\{\chi, \bar{\chi}\}$, respectively.

The twist angle ω_1 in continuum theory relates the untwisted quark mass and the twisted mass by

$$\tan \omega_1 = \frac{\mu_q}{m_q}, \tag{2.8}$$

and is analogously defined in the renormalized theory. The twist angle implies the most interesting feature of tmLQCD. For a twist angle of $\omega_1 = \pi/2$ the theory is referred to be at *maximal twist*. For mtmLQCD (maximal tmLQCD) an automatic $\mathcal{O}(a)$ improvement of physical observables as been shown [3].

The major drawback of the twisted mass formulation of LQCD comes with the twisted mass term $+i\mu\gamma_5\tau_3$. With γ_5 acting in Dirac space and τ_3 acting in flavor space, parity and isospin symmetry are no longer exact symmetries in this lattice formulation. As a consequence a mixing of *parity partners*, states with opposite parity, arises the necessity of dense correlation matrices for a rigorous study of hadrons. The breaking of isospin/flavor symmetry is responsible for a mass splitting in opposite degenerated isospin partners.
With twisted mass at maximal twist, these effects of symmetry breaking are $\mathcal{O}(a^2)$ lattice discretization errors [4, 5] and are going to be investigated in this thesis.

Maximal twist is also applied by realizing the physical quark mass (2.5) only by the twisted mass, as (2.8) shows. This property is fulfilled when the bare untwisted quark mass is tuned to its critical value, so that the untwisted quark mass vanishes

$$m_q = m_0 - m_{\mathrm{crit}}. \tag{2.9}$$

For numerical calculations the Wilson twisted mass QCD action (2.7) will be referred to as

$$S_{\mathrm{F}}[\chi,\bar{\chi},U] = \sum_{x\in\Lambda}\Big(\bar{\chi}(x)(1+i2\kappa a\mu_q\gamma_5\tau_3)\chi(x) \tag{2.10}$$

$$-\kappa\sum_{\mu=0}^{3}\Big[\bar{\chi}(x)U_\mu(x)(1-\gamma_\mu)\chi(x+\hat{\mu}) + \chi(x+\hat{\mu})U_\mu(x)^\dagger(1+\gamma_\mu)\chi(x)\Big]\Big), \tag{2.11}$$

where a rescaled dimensionless fermion field is considered

$$\chi \longrightarrow \frac{\sqrt{2\kappa}}{a^{3/2}}\chi, \quad x_\mu \longrightarrow a\,x_\mu. \tag{2.12}$$

The *hopping parameter* κ is an alternative way of labeling the bare untwisted quark mass and becomes the input variable for numerical calculations

$$\kappa = (2am_0+8)^{-1}. \tag{2.13}$$

For the generation of gauge link configurations the following $N_f = 2+1+1$ twisted mass lattice discretizations were chosen. The lattice action for the light degenerate quark doublet (u,d) is given by [2], corresponding to the introduced formulation of twisted mass LQCD

$$S_{\mathrm{light}}[\chi^{(l)},\bar{\chi}^{(l)},U] = a^4\sum_x \bar{\chi}^{(l)}(x)\left(D_W(m_0) + i\mu\gamma_5\tau_3\right)\chi^{(l)}(x), \tag{2.14}$$

with the quark fields $\chi^{(l)} = \left(\chi^{(u)},\chi^{(d)}\right)$. The *twist transformation*, relating physical and twisted quark fields in the continuum, is given according to (2.4) by

$$\psi^{(l)} = e^{i\omega_l\gamma_5\tau_3/2}\chi^{(l)}, \quad \bar{\psi}^{(l)} = \bar{\chi}^{(l)}e^{i\omega_l\gamma_5\tau_3/2}. \tag{2.15}$$

While for the heavy sea quark doublet non-degenerate quarks (c,s), with a different action according to a proposal by [19] are used

$$S_{\mathrm{heavy}}[\chi^{(h)},\bar{\chi}^{(h)},U] = a^4\sum_x \bar{\chi}^{(h)}(x)\left(D_W(m_0) + i\mu_\sigma\gamma_5\tau_3 + \mu_\delta\tau_1\right)\chi^{(h)}(x), \tag{2.16}$$

where the quark fields denote $\chi^{(h)} = \left(\chi^{(c)},\chi^{(s)}\right)$. This method is based on the flavor off-diagonal splitting $+\mu_\delta\tau_1$ and changes also the twist transformation

$$\psi^{(h)} = e^{i\omega_h\gamma_5\tau_1/2}\chi^{(h)}, \quad \bar{\psi}^{(h)} = \bar{\chi}^{(h)}e^{i\omega_h\gamma_5\tau_1/2}. \tag{2.17}$$

By performing an isovector and axial rotation on (2.16) in the continuum the standard action (2.3) can be achieved with an additional $+\mu_\delta\tau_3$ ($\tau_1 \longrightarrow \tau_3$ due to the vector transformation)

$$S_{\mathrm{F}}[\psi,\bar{\psi},A] = \int \mathrm{d}^4x\;\bar{\psi}(x)\left(\gamma_\mu D_\mu + m + \mu_\delta\tau_3\right)\psi(x). \tag{2.18}$$

The mass of the heavy doublet (c, s) is then described by the split in μ_δ: $m_c = m + \mu_\delta$ and $m_s = m - \mu_\delta$.

In the valence sector of the action a single degenerate quark action, similar to (2.14), will be used. It has been seen [20], that for the *unitary* approach reliable results were difficult to extract in the charm sector, due to a mixing of strange and charm quarks. This problem can be avoided by employing a twisted mass discretization, different from the sea, in the valence sector

$$S_{\text{deg}}[\chi^{(l,c,s)}, \bar{\chi}^{(l,c,s)}, U] = a^4 \sum_x \bar{\chi}^{(l,c,s)}(x) \left(D_W(m_0) + i\mu\gamma_5\tau_3\right) \chi^{(l,c,s)}(x). \tag{2.19}$$

Similar to the light degenerate quark doublet $\chi^{(l)} = \left(\chi^{(u)}, \chi^{(d)}\right)$, strange and charm quarks are described by degenerate twisted mass doublets $\chi^{(c)} = \left(\chi^{(c^+)}, \chi^{(c^-)}\right)$, $\chi^{(s)} = \left(\chi^{(s^+)}, \chi^{(s^-)}\right)$. The degenerate valence doublets allow then two realizations of charm and strange quarks, which differ in the sign of the twisted mass term $\pm i\mu_{c,s}\gamma_5\tau_3$.
This mixed action setup has not only the advantage that a flavor mixing is absent, but also that the valence quarks stay as close to the sea quarks as possible, i.e. the critical mass is identical in the sea and valence sector. Due to the present similarity to the unitary setup this setup will be referred to as unitary setup in the following.

2.1.3 Gauge Action

In the gauge sector the Iwasaki gauge action [21]

$$S_G[U] = \frac{\beta}{3} \sum_x \left(b_0 \sum_{\mu<\nu} \left\{1 - \text{ReTr}\left(U_{\mu\nu}^{1\times1}(x)\right)\right\} + b_1 \sum_{\mu,\nu} \left\{1 - \text{ReTr}\left(U_{\mu\nu}^{1\times2}(x)\right)\right\} \right), \tag{2.20}$$

is adopted, where $\beta = 6/g_0^2$, g_0 being the bare gauge coupling and $b_0 = 1 - 8b_1$ as required for continuum limit normalization, $b_1 = -1/12$ (standard Wilson gauge action for $b_1 = 0$). $U_{\mu\nu}^{1\times1}(x)$ is the plaquette, in the following also referred to as $U_{\mu\nu}(x)$; and $U_{\mu\nu}^{1\times2}(x)$ is a rectangular Wilson loop in the μ-ν-plane.

2.1.4 Mixed action setup

One major aspect of this work is the analysis of lattice discretization errors under use of various lattice actions. Instead of employing different discretizations by generating gauge field configurations a much cheaper option is chosen here: By keeping Wilson twisted mass fermions in the sea and varying only the valence quark action it is possible to achieve early results for observables of interest

$$D_{\text{sea}} \neq D_{\text{valence}}, \quad m_{\text{sea}}^{\text{phys.}} \neq m_{\text{valence}}^{\text{phys.}}, \tag{2.21}$$

where D denotes the Dirac operator. Such an approach is called a mixed action setup. To secure validity within such an approach it is mandatory to relate computed observables

with unitary results, guaranteeing an identical continuum limit convergence of the mixed action setup.

2.1.5 Sea quarks

The sea quark sector describes virtual quark pairs created and annihilated by the gluon field. They appear after Grassmann integration as determinant of the present Dirac operator

$$\langle O \rangle = \frac{1}{Z} \int \mathrm{d}[\chi, \bar{\chi}] \mathrm{d}[U] \; O e^{-S_{\mathrm{eff}}} = \frac{1}{Z} \int [\mathrm{d}U] \; \det \left(D_{\mathrm{sea}}(m_{\mathrm{sea}}) \right) O e^{-S_{\mathrm{G}}}, \tag{2.22}$$

and are highly nontrivial to calculate, since the fermion determinant is a functional of the gauge field (e.g. *quenched approximations*, where these determinants are ignored to simplify the problem).
In a Feynman diagram language sea quark contributions can be referred to as internal closed loops within the hadron, cf. figure 1.

For the sea quark action the Wilson twisted mass discretization presented in section 2.1.2 is adapted. This will not change throughout the work.

2.1.6 Valence quarks

In theory, valence quarks are referred to as those quarks appearing in quark propagators and are so responsible for the quantum numbers of the hadron described

$$D_{\mathrm{valence}}(m_{\mathrm{valence}})^{-1}. \tag{2.23}$$

Referring again to the picture of Feynman diagrams, the valence quark sector can analogously be imagined as the quarks denoted by external and internal lines converging in vertices of the diagram, cf. figure 1.

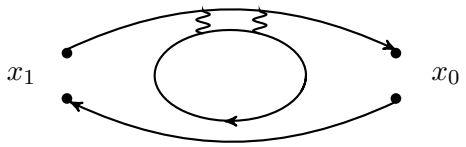

Figure 1: Example of quark lines contributing in mesonic propagators.

As already stated, in contrary to the sea quark action different valence quark actions will be used throughout this work, this corresponds to the computation of quark propagators with valence quark properties. This particular topic will be further discussed in section 3.2.

2.1.7 Symanzik improvement

In a later state of the work the Symanzik improvement programme [22] will be applied on the valence action in order to reduce lattice discretization effects.

For the standard Wilson action, Sheikoleslami and Wohlert have shown that by adding just one extra term to the action an $\mathcal{O}(a)$ on-shell improvement can be achieved. This term is of the same dimension as the leading correction and needs to be multiplied with an appropriate factor, such that next order discretization errors are precisely canceled. By doing so the Wilson action becomes $\mathcal{O}(a)$ improved.
In order to cancel contributions of leading correction writing down the effective lattice action in the form

$$S_{\text{eff}} = \int \mathrm{d}^4x \left(\mathcal{L}^{(0)}(x) + a\mathcal{L}^{(1)}(x) + \mathcal{O}(a^2) \right) \tag{2.24}$$

shows, that therefore an additional term of dimension 5 will be needed. Requiring identical symmetries to the original action $\mathcal{L}^{(0)}(x)$ for the additional term the leading correction term $\mathcal{L}^{(1)}(x)$ can be written as a linear combination $\mathcal{L}^{(1)} = \sum_{j=1}^{5} c_j \mathcal{L}_j^{(1)}$ of five dimension-5 operators.
Application of the Dirac formula allows to omit two of the five operators. Two of the remaining three operators can then be found in the original action and are taken into account by a redefinition of the bare parameters m and g_0. Hence, a single operator is sufficient for the desired $\mathcal{O}(a)$ improvement:

$$S_{\text{clover}}[\chi^{(l)}, \bar{\chi}^{(l)}, U] \quad = \quad c_{\mathsf{sw}} a^5 \sum_{x\in\Lambda} \sum_{\mu<\nu} \bar{\chi}^{(l)}(x) \frac{1}{2} \sigma_{\mu\nu} F_{\mu\nu}(x) \chi^{(l)}(x), \tag{2.25}$$

where $\sigma_{\mu\nu} = i[\gamma_\mu, \gamma_\nu]/2$ and

$$F_{\mu\nu}(x) = \frac{i}{8a^2}(Q_{\mu\nu}(x) - Q_{\nu\mu}(x)) \tag{2.26}$$

is the discretized field strength tensor with

$$Q_{\mu\nu}(x) \equiv U_{\mu\nu}(x) + U_{\nu-\mu}(x) + U_{-\mu-\nu}(x) + U_{-\nu\mu}(x) \tag{2.27}$$

denoting the sum over plaquettes in the μ-ν-plane attached to x, cf. figure 2. Due to the form of $Q_{\mu\nu}$ and its resemblance with a clover leaf, the action in (2.25) is also referred to as clover term.

c_{sw} denotes the above mentioned coefficient, known as *Sheikholeslami-Wohlert coefficient*, which has to be chosen in a suitable way to provide a rigorous elimination of lattice discretization errors.

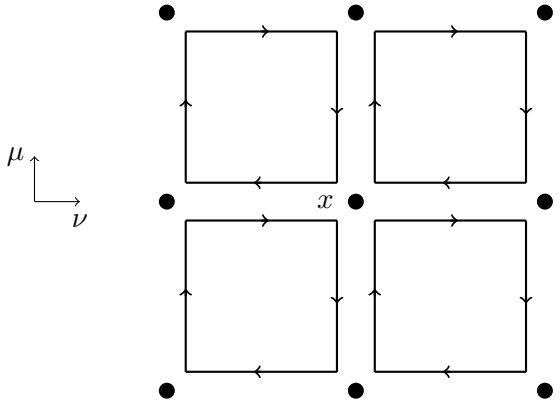

Figure 2: Visualization of the clover leaf structure $Q_{\mu\nu}$ in the μ-ν-plane.

2.2 Effective meson masses on the lattice

This chapter describes how the effective meson masses have been calculated in this work. The procedure for spectroscopy of hadron masses begins with the calculation of quark propagators on given gauge configurations. These are used to calculate correlation functions. A specific structure of gamma matrices is then further applied in the correlation function to compute hadronic states with specific quantum numbers. In the limit of large temporal separation quantities like the mass of the hadron can then be extracted from the correlation function.

2.2.1 The correlation function

The key ingedrient for the calculation of hadron masses is the structure of the hadron correlation function. For a mesonic state with the general form

$$C(t_1 - t_0) = \langle \Omega | \, O_1^\dagger(t_1) O_0(t_0) \, | \Omega \rangle \,, \tag{2.28}$$

where $|\Omega\rangle$ denotes the vacuum. $O(x)$ is a meson interpolator

$$O_j(t) = \frac{1}{\sqrt{\Lambda_3}} \sum_{\mathbf{x} \in \Lambda_3} \bar{\psi}^{(m)}(x) \, \Gamma_j \, \psi^{(n)}(x). \tag{2.29}$$

Γ_j is a product of gamma matrices and has to be chosen with respect to the quantum numbers of the state to be computed. The sum over all lattice sites is necessary for *zero momentum projection*, i.e. $O(t) = O(\mathbf{p} = \mathbf{0}, t)$. The factor $1/\sqrt{\Lambda_3}$ will be omitted in the following.

At zero momentum the analysis of the correlation functions corresponds to an energy equal to the mass of the hadron. Only this allows the Γ's to act as parity projectors, making separate examinations for positive and negative parity contributions possible.

Reordering the fermion fields, with respect to their Grassmann nature, and applying Wick's theorem, i.e. relating the fermionic two-point function with the inverse of the Dirac operator, one rewrites (2.28) into

$$C(t_1 - t_0) = -\mathrm{tr}\left(\sum_{\mathbf{x}_0,\mathbf{x}_1} D^{(n)}(x_0, x_1)^{-1}\gamma_0\Gamma_1^\dagger\gamma_0 D^{(m)}(x_1, x_0)^{-1}\Gamma_0\right), \tag{2.30}$$

where $D^{(m)}(x_1, x_0)^{-1}$ is the inverse Dirac operator. Also referred to as *quark propagator*, since it propagates a quark of flavor (m) from space-time point x_0 to x_1.
Very helpful is the use of the so-called γ_5-*hermiticity* property

$$C(t_1 - t_0) = -\mathrm{tr}\left(\sum_{\mathbf{x}_0,\mathbf{x}_1} \left(D^{(n)}(x_1, x_0)^{-1}\right)^\dagger \gamma_5\gamma_0\Gamma_1^\dagger\gamma_0 D^{(m)}(x_1, x_0)^{-1}\Gamma_0\gamma_5\right). \tag{2.31}$$

Eliminating the need of two separate calculations for the quark propagators when considering identical flavors, and practically giving the backwards running quark propagator for free.
Note that for tmLQCD γ_5-hermiticity comes along with an additional change of the flavor $D^{(u)}(x_0, x_1)^{-1} = \gamma_5\left(D^{(d)}(x_1, x_0)^{-1}\right)^\dagger\gamma_5$, simplifying the calculation of opposite degenerated flavors, e.g. the pion $\bar{\chi}^{(u)}\gamma_5\chi^{(d)}$.

2.2.2 Quark propagators

From the previous section it is clear, that inverting the Dirac operator introduced in (2.19) is mandatory to evaluate correlation functions. However, the quark propagator presented in (2.31) is not calculated. There the entries of $D^{(m)}(x_1, x_0)^{-1}$ build up the connection between every color and Dirac indices of every lattice site. The matrix itself so consists easily of $\mathcal{O}(10^{13})$ complex entries, and is only calculated if possible. As a consequence not only the practical problem to store the complete propagator matrix arises, but also can be found, that the information inside is this huge matrix is correlated.

One possibility of what can be calculated instead is a single column of the full propagator, i.e. by fixing the lattice site. To do so one has to solve the linear system

$$D^{ab}_{AB}(x_2, x_1)\phi_n[\tilde{a}, \tilde{A}, x_0]^b_B(x_1) = \xi_n[\tilde{a}, \tilde{A}, x_0]^a_A(x_2) \tag{2.32}$$

for ϕ, using ξ to fix the site. These spinors are referred to as *sink* and *source* of the quark propagator. For this particular example so-called *point sources* are used, where n denotes the number of the source and $[\tilde{a}, \tilde{A}, x_0]$ denotes the fixed lattice site. In the following this notation will be used to distinguish between the actual indices and space time point of the source ξ (here a, A and x_2) and the lattice site on which the source is located (here $\tilde{a}$, $\tilde{A}$ and x_0). The notation of the fixed lattice site inside the brackets $[\tilde{a}, \tilde{A}, x_0]$ is not strict. This means that the number and order of the indices can vary, as it will be the case in the following section, where only the Dirac indices and the timeslice will be fixed $[\tilde{A}, \tilde{t}]$.

With color and Dirac indices fixed for this particular source type there are in total 12 sources necessary for the inversion of the quark propagator. In general several different methods for the source placement are available, here it gives a propagator for a fixed color and Dirac index, from x_0 to an arbitrary x_1.

$$\phi_n[\tilde{a}, \tilde{A}, x_0]^b_B(x_1) = D^{b\tilde{a}}_{B\tilde{A}}(x_1, x_0)^{-1}. \tag{2.33}$$

This strategy is of course only applicable, if the particular type of sink, constructed be the sources, can be used to express the requested correlation function.

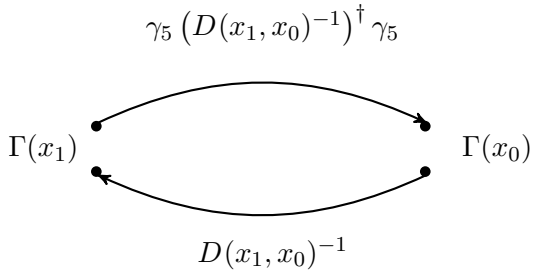

Figure 3: Visualization of the quark propagator connecting source and sink.

2.2.3 Spin diluted timeslice sources and the one-end trick

With a great reduction of the noise-to-signal ratio over other stochastic methods (cf. e.g. [23]) spin diluted timeslice sources in combination with the *one-end trick* (cf. e.g. [24]) are applied throughout this work. There the stochastic noise vanishes entirely on one end of the correlator.
Beginning with the introduction of random *spin diluted* timeslice sources

$$\xi_n[\tilde{A}, \tilde{t}]^a_A(x) = \delta_{A,\tilde{A}}\delta(t - \tilde{t}) \left(\pm\frac{1}{\sqrt{2}} \pm \frac{i}{\sqrt{2}}\right), \tag{2.34}$$

$3 \times \Lambda_3$ random complex numbers are generated and copied to four sources n, where they appear in different Dirac components. As a consequence four separate inversions are needed on every gauge configuration for the chosen timeslice, to calculate the complete number of Dirac indices.
A different choice for the stochastic noise is possible as well, as long as

$$\left\langle \left(\xi_n[\tilde{A}, \tilde{t}]^a_A(x)\right)^\dagger \xi_n[\tilde{B}, \tilde{t}]^b_B(y) \right\rangle = \delta^{a,b}\delta_{A,\tilde{A}}\delta_{B,\tilde{B}}\delta(\mathrm{x}_0 - \tilde{t})\delta(\mathrm{y}_0 - \tilde{t})\delta(\mathbf{x} - \mathbf{y}) \tag{2.35}$$

is fulfilled. The brackets in $\langle \xi^\dagger \xi \rangle$ denote the average of an infinite number of samples.

In a subsequent step the actual inversion of the lattice Dirac operator for the given sample source has to be performed, i.e. solving $D\phi = \xi$ for ϕ

$$\phi_n[\tilde{A},\tilde{t}]^b_B(x_1) = \sum_{x_0} D^{ba}_{BA}(x_1,x_0)^{-1}\xi_n[\tilde{A},\tilde{t}]^a_A(x_0). \tag{2.36}$$

This is very CPU time expensive, especially for light quark masses. The operations were performed by using an iterative solver (here: conjugated gradient method) implemented in the tmLQCD package. For a more detailed discussion of the technical realization consider [25, 26].

After the inversion of the Dirac operator the meson correlation function is computed according to (2.31).
Without the use of spin diluted sources one quickly finds a limitation to a certain Γ structure, taking into account that spinors are used for the quark propagation

$$C(t_1-t_0) = -\left\langle \sum_{\mathbf{x_1}} \phi_n[\tilde{A},\tilde{t}]^a_A(x_1)^\dagger \Gamma_{AB} \phi_n[\tilde{B},\tilde{t}]^b_B(x_1) \right\rangle \tag{2.37}$$

$$= -\Bigg\langle \sum_{\mathbf{x_0},\mathbf{x_1},\mathbf{x_2}} \left(\xi_n[\tilde{A},\tilde{t}]^c_C(x_0)\right)^\dagger \left(D^{ca}_{CA}(x_1,x_0)^{-1}\right)^\dagger \Gamma_{AB} D^{bd}_{BD}(x_1,x_2)^{-1}\xi_n[\tilde{B},\tilde{t}]^d_D(x_2) \Bigg\rangle \tag{2.38}$$

$$= -\mathrm{tr}\left(\sum_{\mathbf{x_0},\mathbf{x_1}} \left(D(x_1,x_0)^{-1}\right)^\dagger \Gamma D(x_1,x_0)^{-1} \right). \tag{2.39}$$

This provides the requested correlation function (2.31) only for $\Gamma = \gamma_5\gamma_0\Gamma_1^\dagger\gamma_0$ and under a restriction of the corresponding $\Gamma_0 = \gamma_5$.

Using the concept of spin dilution a second Γ can be implemented in (2.37)

$$C(t_1-t_0) = -\left(\Gamma_0\gamma_5\right)_{FE} \left\langle \sum_{\mathbf{x_1}} \phi_n[E,t_0]^a_A(x_1)^\dagger \left(\gamma_5\gamma_0\Gamma_1^\dagger\gamma_0\right)_{AB} \phi_n[F,t_0]^b_B(x_1) \right\rangle \tag{2.40}$$

$$= -\left(\Gamma_0\gamma_5\right)_{FE} \Bigg\langle \sum_{\mathbf{x_0},\mathbf{x_1},\mathbf{x_2}} \left(\xi_n[E,t_0]^c_C(x_0)\right)^\dagger \left(D^{ca}_{CA}(x_1,x_0)^{-1}\right)^\dagger \left(\gamma_5\gamma_0\Gamma_1^\dagger\gamma_0\right)_{AB} D^{bd}_{BD}(x_1,x_2)^{-1}\xi_n[F,t_0]^d_D(x_2) \Bigg\rangle \tag{2.41}$$

$$= -\sum_{\mathbf{x_0},\mathbf{x_1}} \left(\Gamma_0\gamma_5\right)_{FE} \left(D^{ca}_{EA}(x_1,x_0)^{-1}\right)^\dagger \left(\gamma_5\gamma_0\Gamma_1\gamma_0\right)_{AB} D^{bd}_{BF}(x_1,x_0)^{-1}. \tag{2.42}$$

As it can be seen, the correlation function (2.31) is successfully rebuilt in the case of spin diluted timeslice sources.

2.2.4 Calculation of effective meson masses

The correlation function can then be used to extract the corresponding meson mass. Adopting the limit $T \to \infty$ the correlation function, written in the basis of eigenstates of the hamiltonian $\hat{H}$, quickly reduces to

$$C(t_1 - t_0) = \langle \Omega | \, O_1^\dagger(t_1) O_0(t_0) \, | \Omega \rangle \tag{2.43}$$

$$= \sum_k \langle \Omega | O_1(t_1)^\dagger | k \rangle \langle k | O_0(t_0) | \Omega \rangle e^{-(E_k - E_\Omega)\Delta t}, \tag{2.44}$$

with $|\Omega\rangle$ as vacuum state and E_Ω as vacuum energy.
It can be seen that low lying states at large temporal separation have a dominating contribution. The effective mass can be extracted by taking

$$m_{\text{eff}} = \ln \left(\frac{C(t)}{C(t+a)} \right) \tag{2.45}$$

In the limit $t \to \infty$ only ground state contributions will remain, giving the mass of the particular state

$$m_{\text{meson}} = \lim_{t \to \infty} \ln \left(\frac{C(t)}{C(t+a)} \right) = E_1 - E_\Omega. \tag{2.46}$$

However, this work is concerned with the investigation of excited states. As already mentioned due to parity symmetry breaking positive parity partners suffer from mixing contributions from negative partners and vice versa. To study such states the calculation of correlation matrices is necessary

$$C_{jk}(t) = \langle \Omega | \, O_j^\dagger(t) O_k(0) \, | \Omega \rangle \, . \tag{2.47}$$

C_{jk} is a $N \times N$ matrix that describes N different states, where for Wilson twisted mass the parity mixing contributions between operators are located on their off-diagonal elements. Effective masses of all N states have to be extracted in one single operation, i.e. by solving the generalized eigenvalue problem

$$C_{jk}(t) v_k^{(n)}(t, t_0) \quad = \quad C_{jk}(t_0) v_k^{(n)}(t, t_0) \lambda^{(n)}(t, t_0), \quad n = 1, ..., N \quad t > t_0, \tag{2.48}$$

(cf. e.g. [27]). Similar to the previous case the effective mass is obtained by analyzing exponentials of the eigenvalues

$$m_{\text{eff}}^{(n)}(t, t_0) \quad = \quad \ln \left(\frac{\lambda^{(n)}(t, t_0)}{\lambda^{(n)}(t + a, t_0)} \right). \tag{2.49}$$

In the limit $t \to \infty$ the effective mass will again yield the mass of the n-th state observed.

To assign the observed masses to the interpolators, an evaluation of the squared absolute value of the eigenvector components $|v_k^{(n)}|^2$ is additionally needed. Especially for more complex problems with several interpolators, only the functional behavior of $|v_k^{(n)}|^2$ in temporal separation reveals contributions to the observed masses from the n different states.

Considering a finite temporal lattice site T, meson propagation in t is symmetric in $T-t$. This can be found in a proportionality of the eigenvalues $\lambda^{(n)}(t,t_0) \sim e^{-E_n t} + e^{-E_n(T-t)}$, so that with (2.49) and

$$\frac{\lambda^{(n)}(t,t_0)}{\lambda^{(n)}(t+a,t_0)} = \frac{e^{-E_n t} + e^{-E_n(T-t)}}{e^{-E_n(t+a)} + e^{-E_n(T-(t+a))}} \tag{2.50}$$

a cosh dependence in the effective mass plateau can be found. Due to that all effective mass plateaus will be shown for $t/a < T/2a - 1$.

3 Numerical results

3.1 Simulation setup

All results are based on gauge configurations generated by the ETM (European Twisted Mass) collaboration, with Iwasaki gauge action (2.20) and $N_f = 2 + 1 + 1$ flavors of twisted mass quarks (2.14), (2.16).

The fermionic and gauge sector of the action were presented in section 2.1.2.
Details to the Ensemble that was used are found in table 1.

Ensemble	β	$(L/a)^3 \times (T/a)$	κ	$a\mu$	$a\mu_\sigma$	$a\mu_\delta$
A40.32	1.9	$32^3 \times 64$	0.16327	0.004	0.15	0.19

Table 1: Summary of the ensemble parameters.

This corresponds to a lattice spacing $a \approx 0.086$ fm and a pion mass $m_\pi \approx 320$ MeV.
For more details, consider [28]. All computations in this work have been performed on ≈100 gauge link configurations.

3.2 Tuning of the valence sector

3.2.1 Wilson twisted mass valence quarks

Following the introduction of section 2.1.2 this action setup is not a unitary setup, but the closest mixed action setup to it, hence it will be referred to as unitary approach in the following. This setup is commonly used in the ETM collaboration, e.g. for the computation of the spectrum of meson masses, cf. [9, 10]. As a consequence of the lattice discretization errors in the Wilson twisted mass approach the spectroscopy of several meson masses become more complicated.
This works main purpose is the investigation of three lattice discretizations different from the unitary approach (cf. the following sections) with the expectation of finding an action setup, that may provide more suitable conditions for the spectroscopy of meson masses. In the most ideal case the advantages of both actions from the sea and the valence would be found to be combined for the computation.
This valence sector will so mainly serve as a reference point for every calculated observable and so help to analyze the effectiveness of the chosen strategy to reduce lattice discretization effects.

In the valence sector the critical hopping parameter is identical to the sea with $\kappa_{\text{crit}} = (2am_{\text{crit}}+8)^{-1} = 0.16327$ and also is the light quark mass $a\mu_l = 0.004$. The corresponding strange and charm masses are $a\mu_s = 0.02322$ and $a\mu_c = 0.27678$, such that the K and

D meson mass within the mixed action setup with structure $\bar{s}^{+}d$ and $\bar{c}^{+}d$, correspond to the unitary K and D meson mass [20], i.e. using (2.19) for computation of valence quarks.
The complete lattice action can be written as

$$S_{\text{tm valence}}[\chi, \bar{\chi}, U] = S_{\text{deg}}[\chi, \bar{\chi}, U] + S_{\text{G}}[U]. \tag{3.1}$$

3.2.2 Wilson valence quarks

Since the standard Wilson action is by itself not improved, and thus suffers from $\mathcal{O}(a)$ discretization effects, results obtained in this mixed action setup are not expected to be qualitatively on the level of the other setups. Nevertheless as an intermediate step, before improving the Wilson fermions with the use of the clover term, numerical results will be presented here and serve later as an additional reference for the Wilson clover results.

To compute Wilson valence quarks on the twisted mass sea, the degenerate Wilson twisted mass lattice action (2.19) will be used as valence action. By setting the twisted mass term to zero, i.e. $a\mu = 0$, the Dirac operator is identical to the standard Wilson operator and the twist transformations, which related the physical quark fields to the twisted quark fields, can be omitted, since quark fields will directly be used in the physical basis, i.e. $\chi^{(f)} \to \psi^{(f)}$.

When using a Wilson valence action, advantages are encountered during the computation of correlation matrices. Since parity and isospin symmetries are exact for a Wilson action, no parity and isospin discretization errors are expected at all. Parity partner are thus free from off-diagonal elements, i.e. $C_{jk} = 0$ for $j \neq k$ while calculating a correlation matrix. This feature might be of considerable advantage when one wants to calculate correlation matrices which rely on sizable HPC resources.

Without the need for a parameter ensuring maximal twist the hopping parameter will determine quark masses in the Wilson valence sector. The light and charm hopping parameter $\kappa_l = 0.162214$ and $\kappa_c = 0.13582$ have been tuned such that the pion and D meson mass, with structure $\bar{u}d$ and $\bar{c}d$, are approximately the same as for Wilson twisted mass valence quarks, cf. 3.2.1.
The complete lattice action can be written as

$$S_{\text{Wilson valence}}[\psi, \bar{\psi}, U] = S_{\text{deg}}^{\mu=0}[\psi, \bar{\psi}, U] + S_{\text{G}}[U]. \tag{3.2}$$

3.2.3 Wilson + clover valence quarks

Here a similar procedure as in the previous setup is adopted. By now adding the clover action (2.25) to the standard Wilson valence action (2.19), where $a\mu = 0$, lattice discretization errors of $\mathcal{O}(a)$ can be canceled. The Sheikoleslami Wohlert coefficient c_{sw} is chosen according to a perturbative expansion [29]

$$c_{\mathsf{sw}}(g_0) = 1 + c_{\mathsf{sw}}^{(1)} \frac{g_0^2}{\langle U_{\mu\nu} \rangle} + \mathcal{O}(g_0^4). \tag{3.3}$$

$c_{\mathsf{sw}}(0) = 1$ being the tree-level value for all gauge actions.
There the coefficient $c_{\mathsf{sw}}^{(1)}$ was determined for several ensembles, for an ensemble as used in this work it was found that $c_{\mathsf{sw}}^{(1)} = 0.113(3)$. Together with an average plaquette value of $\langle U_{\mu\nu} \rangle = 0.575079$ we find for our setup

$$c_{\mathsf{sw}} = 1.62051. \tag{3.4}$$

Tuning of the light and charm hopping parameter is done analogously to the previous setup. Note the reduction in the absolute value of the hopping parameter due to the addition of the clover term. It is found $\kappa_l = 0.13832$ and $\kappa_c = 0.12286$.
The complete lattice action can be written as

$$S_{\text{Wilson+clover valence}}[\psi, \bar{\psi}, U] = S_{\text{deg}}^{\mu=0}[\psi, \bar{\psi}, U] + S_{\text{clover}}[\psi, \bar{\psi}, U] + S_{\text{G}}[U]. \tag{3.5}$$

3.2.4 Wilson twisted mass + clover valence quarks

In the last considered mixed action setup the clover action is added to the Wilson twisted mass action as present in 3.2.1. This approach may at first appear odd, since we know that Wilson twisted mass is already automatic $\mathcal{O}(a)$ improved at maximal twist by itself, and the clover improvement was initially designed for a standard Wilson action in order to cancel $\mathcal{O}(a)$ errors. But it is implied in [7], that adding the clover term to a maximal twisted Wilson twisted mass action could result in an improved $\mathcal{O}(a^2)$ behavior ($\mathcal{O}(a^2)$ contributions may not vanish, but are supposed to be reduced compared to Wilson twisted mass).

The c_{sw} coefficient (3.4) is kept for this setup. However, by adding the clover term to our Wilson twisted mass action, maximal twist realized as previously is not guaranteed to be still valid. Instead we find that the theory is not at maximal twist anymore and so an additional retuning of parameters is required here.

To restore maximal twist the method of setting m_{PCAC} to zero was applied. The PCAC (partially conserved axial current) mass is by renormalization constants related to the untwisted quark mass. Evaluating a vanishing PCAC mass for a large enough temporal separation is hence in agreement with a bare untwisted quark mass at its critical value,

i.e. the theory at maximal twist. The tuning has been performed by adjusting κ such that the PCAC mass vanishes in the light quark sector,

$$m_{\mathrm{PCAC}} = \frac{\sum_x \langle \partial_0 A_0^a(x) P^a(0) \rangle}{2 \sum_x \langle P^a(x) P(0) \rangle}, \qquad a = 1, 2, \tag{3.6}$$

where

$$A_\mu^a(x) = \frac{1}{2} \bar{\chi}^{(l)}(x) \gamma_\mu \gamma_5 \tau^a \chi^{(l)}(x), \quad P^a(x) = \frac{1}{2} \bar{\chi}^{(l)}(x) \gamma_5 \tau^a \chi^{(l)}(x), \tag{3.7}$$

are the axial vector current and the pseudo scalar density, respectively.

Figure 4 shows the tuning process of am_{PCAC} for this particular c_{sw}. The considered slope in $1/2\kappa$ was set to 1.0 by default and as it can be seen, applied with great agreement to the situation. With a value of

$$am_{\mathrm{PCAC}} = -1.23 \cdot 10^{-4} \pm 1.15 \cdot 10^{-4} \tag{3.8}$$

the PCAC mass was determined in a demanded range of $|m_{\mathrm{PCAC}}|/\mu \leq 0.1$ (where $\mu = 0.004$), a criterion commonly used for the tuning to maximal twist, e.g. [28].

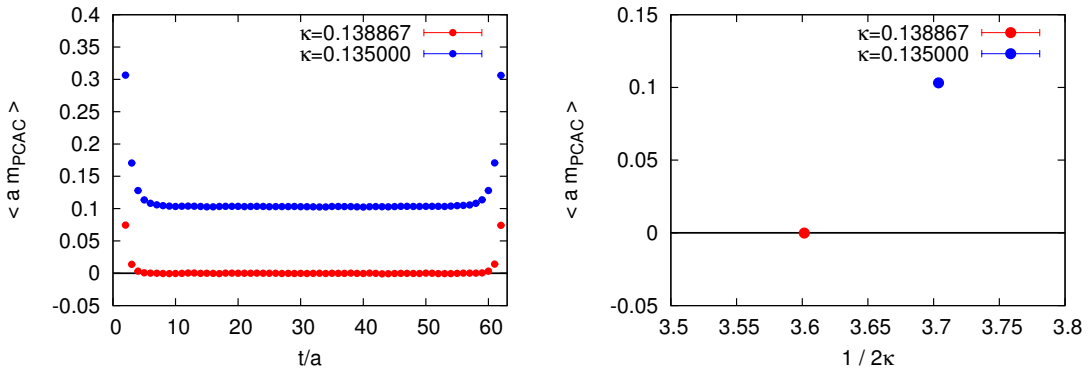

Figure 4: Tuning of am_{PCAC} for $c_{\mathrm{sw}} = 1.62051$. (left) am_{PCAC} as a function of temporal seperation; (right) am_{PCAC} as function of $1/2\kappa$. The slope for am_{PCAC} in $1/2\kappa$ is 1.0 in this case.

Maximal twist was found to be restored for a critical hopping parameter of $\kappa = 0.138867$. After applying the clover term to the Wilson twisted mass action and retuning to maximal twist, unitary results are not immediately restored. Instead further tuning in the quark mass parameter μ are necessary to adjust the masses in a rather small range. Here a slight shift of the dependency between pseudo scalar masses and quark masses can be observed. m_{PS} in the light quark sector becomes heavier while the pseudo scalar mass in the heavy quark sector becomes lighter, than in a setup without clover term. For a

more detailed study regarding this behavior consider [5]. So tuning of quark masses for the light and charm quark mass develops in different directions in $a\mu$, cf. figure 5.

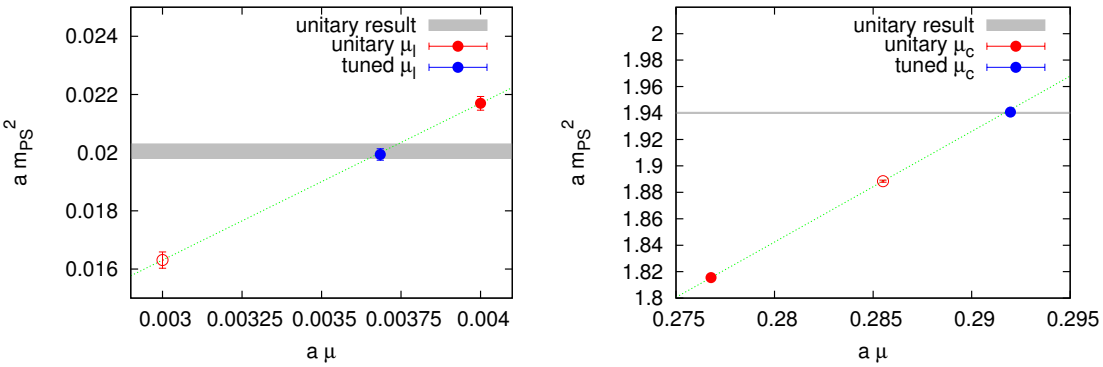

Figure 5: Tuning of the quark mass parameter μ with a constant $\kappa = 0.138867$ for the light (left) and charm (right) quark mass with linear behavior in the pseudo scalar mass squared. Notice the opposite directory of the shift between the unitary and the tuned μ in the light and heavy sector.

The light and charm quark masses $a\mu_l = 0.003685$ and $a\mu_c = 0.291968$ approximately restore the pion and the D meson mass as given in the unitary setup.
The complete lattice action can be written as

$$S_{\text{tm+clover valence}}[\chi, \bar{\chi}, U] = S_{\text{deg}}[\chi, \bar{\chi}, U] + S_{\text{clover}}[\chi, \bar{\chi}, U] + S_{\text{G}}[U]. \tag{3.9}$$

To summarize all tuning parameters for the four different mixed action approaches, presented throughout this section, an overview of the tuned hopping parameters and quark masses can be found in table 2.

	Wilson twisted mass	
	without clover	with clover
κ_{crit}	0.16327	0.138867
$a\mu_l$	0.0040	0.003685
$a\mu_c$	0.27678	0.291968

	Standard Wilson	
	without clover	with clover
κ_l	0.162214	0.13832
κ_c	0.13582	0.12286

Table 2: Input parameters for both Wilson twisted mass and Wilson valence quarks, with and without a clover term where $c_{\text{sw}} = 1.62051$.

3.3 Effective meson masses

The results presented here are produced by application of the one-end trick as explained in section 2.2.3. For each stochastic timeslice source the timeslice was chosen randomly for every gauge field configuration.
Inversion of the Dirac propagator was performed with a precision of $\epsilon^2 = 10^{-18}$, referring to a stopping criterium for the iterative solver, where the squared norm of the residual propagator has to fulfill a precision of $||r||^2 < \epsilon^2$.

In order to extract mass values for the computed mesons χ^2 minimizing fits of a constant are performed to the corresponding mass plateaus. As a criterion on the quality of the fit $\chi^2/\mathrm{dof} \lesssim 2.0$ is required. Fitting intervals $[t_{\min}/a, t_{\max}/a]$ are chosen for $t_{\max}/a \leq 25$, see (2.50), briefly below the symmetric point. Pseudo scalar masses, with rather nice plateaus, are usually fitted in a range of $[t_{\min}/a, t_{\max}/a] = [15, 25]$.
$t_{\max}/a$ for scalar masses is chosen as a cut off for effective masses on ascendent temporal separations, that suffer from too much noise.

Table 3 summarizes the mesonic states and the corresponding operators that are used for the following calculations.

Meson	Operator	J^P
$\pi^{\pm}$, $\pi^{0,\mathrm{con}}$	$\bar{\chi}^{(u)}\gamma_5\chi^{(d)}$, $\bar{\chi}^{(u)}\chi^{(u)} + \bar{\chi}^{(d)}\chi^{(d)}$	0^-, 0^-
D, D_0^*	$\bar{\chi}^{(c^+)}\gamma_5\chi^{(d)}$, $\bar{\chi}^{(c^+)}\chi^{(d)}$	0^-, 0^+
J/ψ, h_c	$\bar{\chi}^{(c^+)}\gamma_j\gamma_5\chi^{(c^-)}$, $\bar{\chi}^{(c^+)}\gamma_j\chi^{(c^-)}$	1^-, 1^+
	$\bar{\chi}^{(c^-)}\gamma_j\chi^{(c^-)}$, $\bar{\chi}^{(c^-)}\gamma_j\gamma_5\chi^{(c^-)}$	1^-, 1^+

Table 3: Mesonic states and their quantum numbers that were calculated within this work. The operators are presented for twisted mass fields with two degenerate quarks, $j \in \{1, 2, 3\}$.

3.3.1 Light quark mass tuning

Tuning of the light quark masses may have been the most time-consuming part of the whole work, considering the very CPU-time expensive operations of Dirac operator inversions. In figure 6 the time that was needed to find a solution with the conjugated gradient method is shown. Every dot represents the inversion of a single source, where for one gauge field configuration four sources are needed to be inverted, due to the one-end trick.

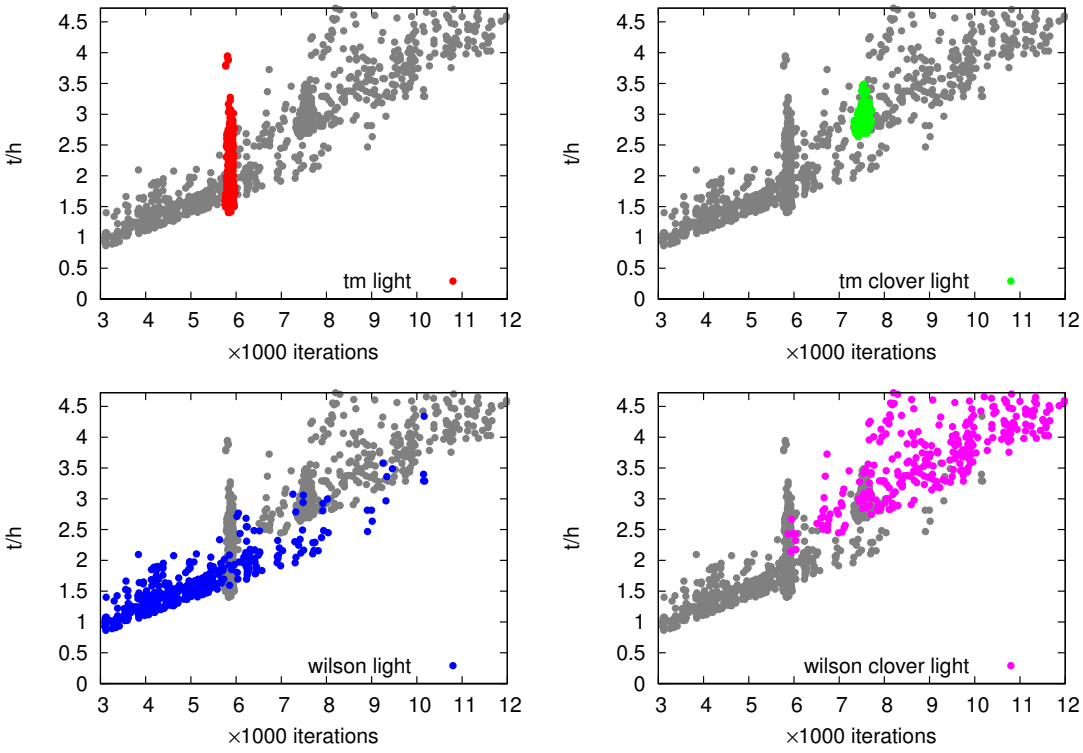

Figure 6: CPU-time for the inversion of a light quark mass Dirac operator over the number of iterations needed to find a minimum with the conjugated gradient method for identical precision in all setups.

In figure 7, the tuning results of the pion mass is presented, for three of the four mixed action setups. Twisted mass results show excellent mass plateaus for the pion, with minor fluctuations after addition of the clover term.
However, light quark masses in the Wilson valence action show already an increase in the statistical noise for $t \gg a$, even if the errors are still small. After addition of the clover term to the action the picture gets worse. It was found that for Wilson+clover valence quarks the mass plateau can not be determined via the same procedure as in the previous cases. Large noise contributions already at small temporal separations make it close to impossible to get a clear picture of a plateau. This behavior shows up when approaching the light quark mass for an increasing hopping parameter κ. Where there are still smooth plateaus for a pion mass around $2am_{\pi^\pm}$ and above, and increasing error in the plateau value for a decreasing pion mass already suggests a change for the worse of the studied case. Below $2am_{\mathrm{PS}}$ the picture changes drastically, so that a plateau can not be found.

Reason for this behavior can be concluded from the critical hopping parameter κ_{crit} of the Wilson twisted mass + clover valence action. As can be seen from table 2 the absolute value of $\kappa_{\text{l}} = 0.13832$ for Wilson + clover has to be chosen noticeable close to the value for which the theory with clover term is at maximal twist, i.e. $\kappa_{\text{crit}} = 0.138867$. So the Wilson + clover valence action approximately corresponds to the theory at maximal twist with $\mu = 0$. Omitting the mass-like contributions coming from the application of the clover term this would in principle mean to compute pion masses below the unitary value. The situation is similar for the setup without the clover term, where $\kappa_{\text{crit}} = 0.16327$ and $\kappa_{\text{l}} = 0.162214$, but the hopping parameter for light quark masses is separated enough from the critical value, such that still mass plateaus can be computed.

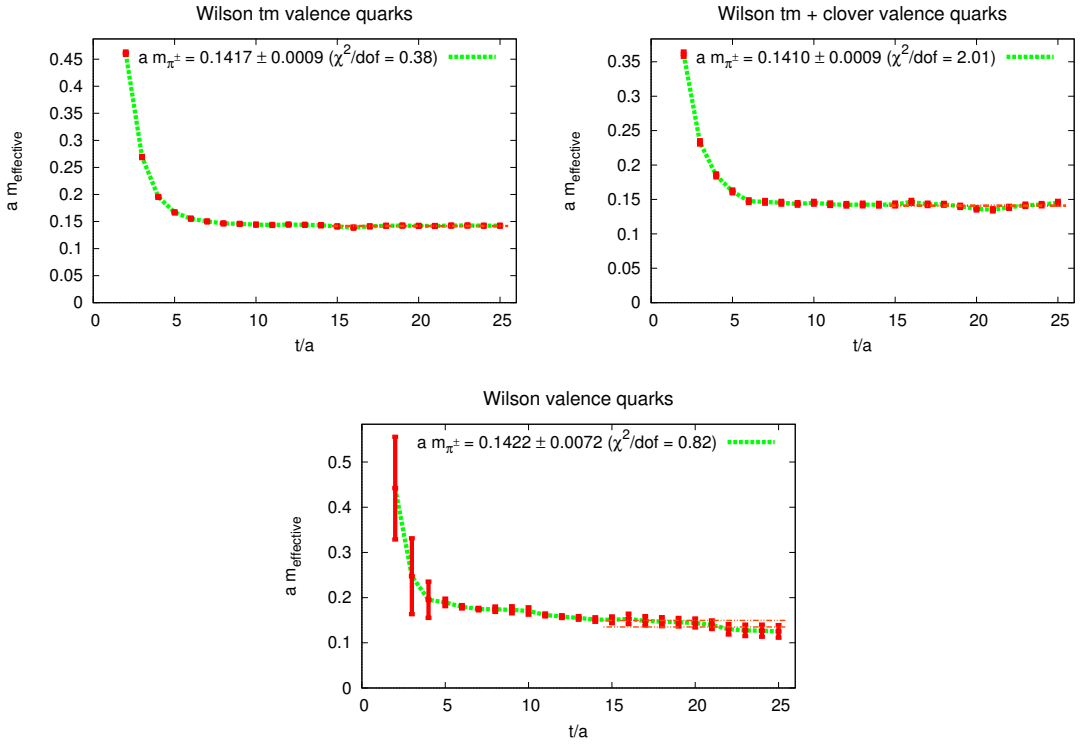

Figure 7: Effective masses for the pion in all mixed action setups. The pion mass $am_{\pi^\pm}$ was demanded to be identical within errors.

The corresponding light hopping parameter for the Wilson action setup with clover term is then determined by an extrapolation of the pion mass in $1/2\kappa$, with use of the clear mass plateaus values above, cf. figure 8.
The following purpose of the tuned light quark mass is to tune the charm quark mass parameters such that the corresponding D meson masses is consistent within all mixed action setups. Since the mass of the D meson is mostly composed of charm quark

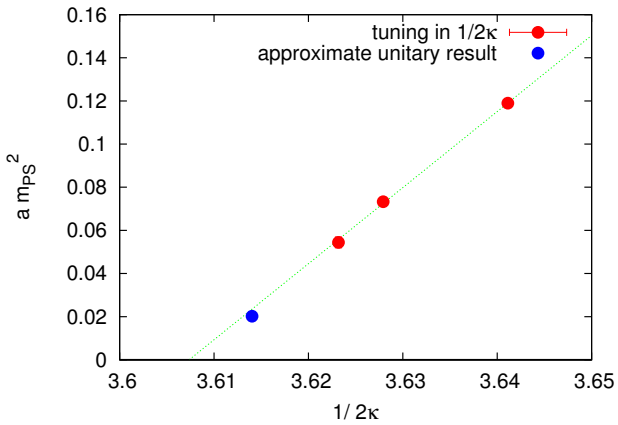

Figure 8: Pion masses in the Wilson+clover action setup. Extrapolation leads to the hopping parameter used for the simulation of a light quark mass corresponding to m_{PS} of the Wilson twisted mass action setup.

contributions, displacements of the pion mass affect the D mass value only in a very mild way, hopefully suppressing the effects coming from the inability to produce a clear mass plateau for Wilson+clover. Figure 9 shows agreement within errors for the D meson mass in several charm quark masses with an altered light quark mass of $1.3m_{\pi^{\pm}}$ in the setup with Wilson valence quarks. This argument is obviously valid independent of the action of choice.

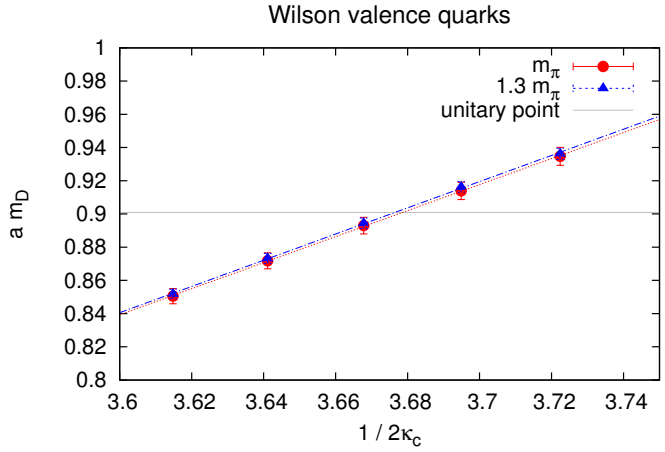

Figure 9: D meson mass for five different charm quark masses and two light quark masses separated by 30%. Change of the charm quark mass shows distinct changes in contrast to the light quark mass.

3.3.2 Calculation of effective D, D_0^* masses

After tuning the light quark mass parameter to unitary results it is possible to determine the charm quark mass for every setup, using a similar procedure. Instead of using pseudo scalar mass results for the charm quark the D meson was chosen, with an already tuned light quark component, to determine the charm quark parameter.
The mass of the parity partner D_0^* -which resulted from every setup individually, i.e. no additional tuning is necessary- allowed then a first study of the discretization effects. Effective masses of the D and D_0^* meson are shown in figure 10.

Relating to (2.47) the operators used are $O_j \in \{\bar{\chi}^{(c^+)}\gamma_5\chi^{(d)}, \bar{\chi}^{(c^+)}\chi^{(d)}\}$ for both Wilson twisted mass valence quarks, and $O_j \in \{\bar{\psi}^{(c)}\gamma_5\psi^{(d)}, \bar{\psi}^{(c)}\psi^{(d)}\}$ for Wilson valence quarks. This way operators generate the D and D_0^* meson with respective quantum numbers of $J^P = 0^-$ and $J^P = 0^+$, when applied to the vacuum.

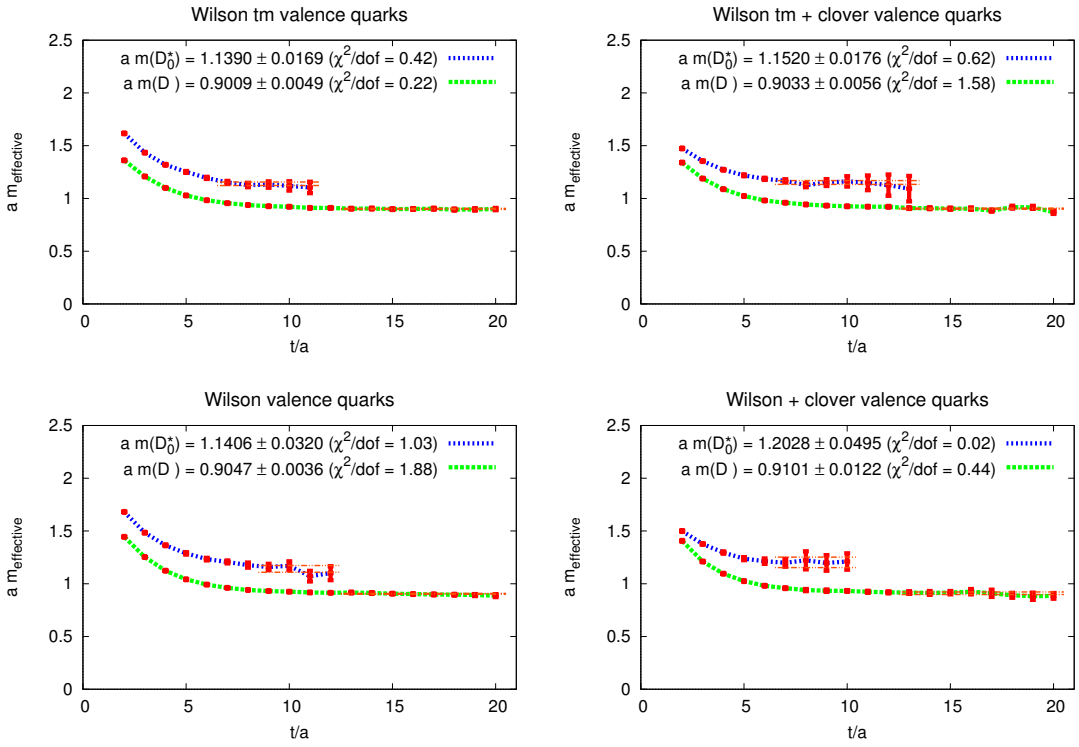

Figure 10: Effective masses of the D and D_0^* meson, obtained in four mixed action setups, as a function of temporal separation t/a.

The mass of the low lying parity partner is identical within the setups by construction and thus not of interest regarding further interpretations of the acquired results. The quality of the plateau value is similar within all the setups except for the Wilson+clover

setup, with a slightly worse picture.

For the excited D_0^* state one can observed that Wilson twisted mass valence quarks, regardless of a present clover term, yield plateau values in a similar error range, which is not the case for the plateau values of both Wilson valence quarks. There the addition of the clover term apparently even worsens the picture. In contrast to the Wilson twisted mass valence quarks the clover term even shortens the temporal separation of the effective mass plateau, an additional effect that is a reason for the worse plateau value.

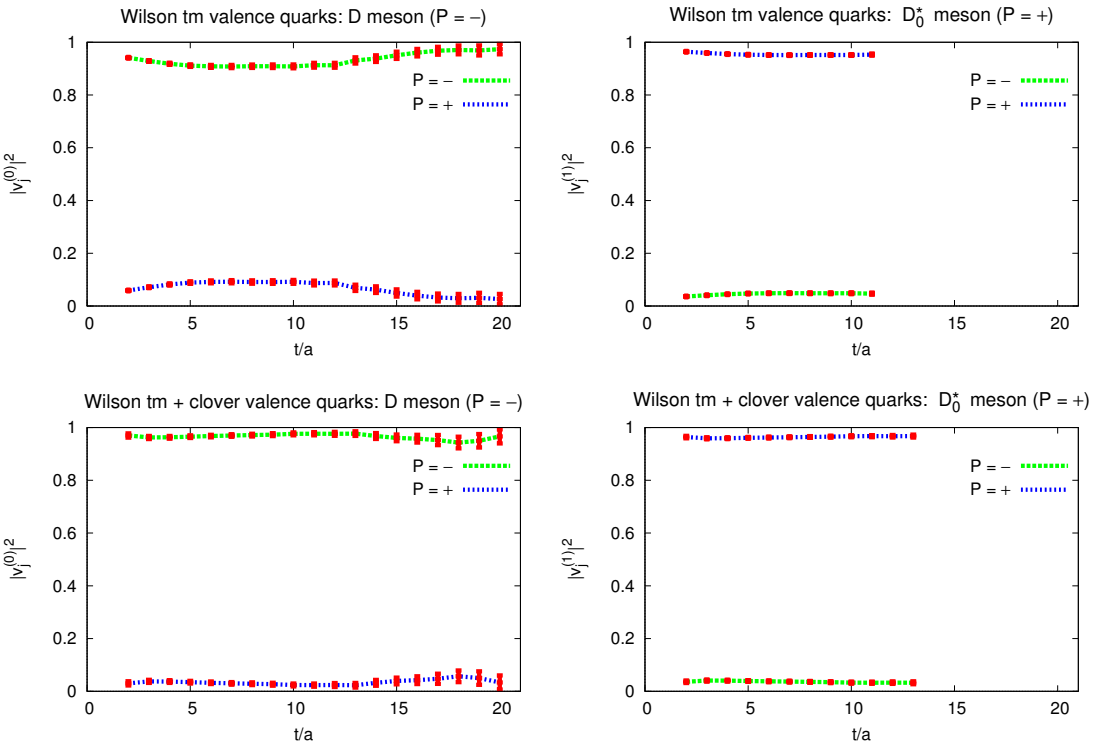

Figure 11: Squared absolute eigenvector components for the D and D_0^* meson for Wilson twisted mass valence quarks, with and without clover term. Column line graphs show the behavior for states of equal parity.

The squared absolute eigenvector components $|v_j^{(n)}|^2$ of the generalized eigenvalue problem (2.48) as function of temporal separation t/a are shown in figure 11. For Wilson valence quarks no eigenvector components are shown. With parity as an exact symmetry in this action setup no off-diagnoal elements are present in the correlation matrix, eliminating parity mixing between the low lying and excited state entirely.

It is observed that for the $P = -$ state indeed a reduction of parity mixing between the $P = -$ and $P = +$ state from around $\lesssim 10\%$ down to $< 5\%$ is present. On the other hand, no further significant improvement for the parity mixing of the $P = +$ state has been observed.

3.3.3 Calculation of effective J/ψ, h_c masses

Spectroscopy of the effective masses of the J/ψ meson and its parity partner h_c are done in a complete analogous way to the previous section.
The flavor neutral η_c and its parity partner χ_{c0} are not studied, since even for twisted mass fermions no parity mixing is present for these operators.

The operators used are $O_j \in \{\bar{\chi}^{(c^+)}\gamma_k\gamma_5\chi^{(c^-)},\ \bar{\chi}^{(c^+)}\gamma_k\chi^{(c^-)}\}$ for both Wilson twisted mass valence quarks, and $O_j \in \{\bar{\psi}^{(c)}\gamma_k\psi^{(c)},\ \bar{\psi}^{(c)}\gamma_k\gamma_5\psi^{(c)}\}$ for Wilson valence quarks, with $k \in \{1, 2, 3\}$, generating the quantum numbers of $J^P = 1^-$ and $J^P = 1^+$, when applied to the vacuum.

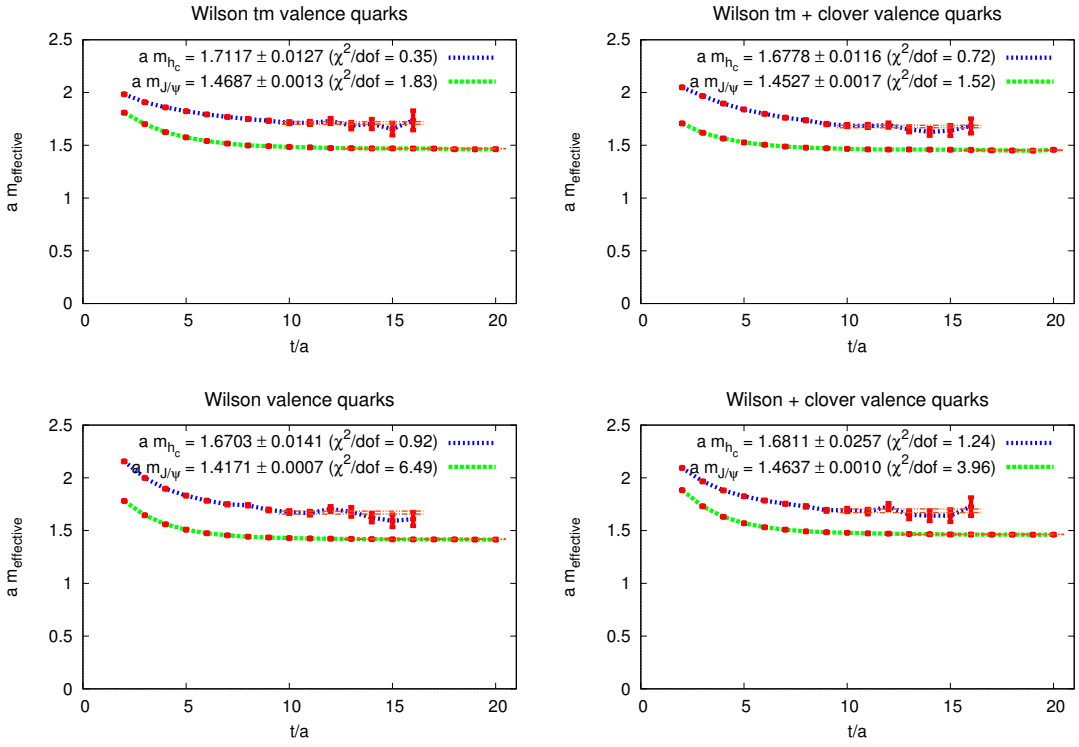

Figure 12: Effective masses of the J/ψ and h_c meson, obtained in four mixed action setups, as a function of temporal separation t/a.

Figure 12 shows the effective mass plots for all mixed action setups, where a similar behavior as for the already observed D and D_0^* can be noted. Pseudo vector mass fits remain to give a very clear picture of the state. With a noticeable difference of the absolute mass value for Wilson valence quarks the unimproved $\mathcal{O}(a)$ theory stands out from the others. This may be an indication for the $\mathcal{O}(a)$-improvement in the other setups. However, in case of Wilson valence quarks (with and without additional clover term) the initial criterion of $\chi^2/\mathrm{dof} \lesssim 2.0$ is not possible to be fulfilled.
A benefit in terms of a decrease in the statistical error for vector states is not observed after the addition of the clover term. It appears that every action setup produces a similar width in the temporal separation of the plateau, so that no more worsening in the width for Wilson valence quarks remains present. The error range of the plateau value fit is now approximately equal within three of the four setups, only Wilson valence quarks with clover term remain somewhat above.

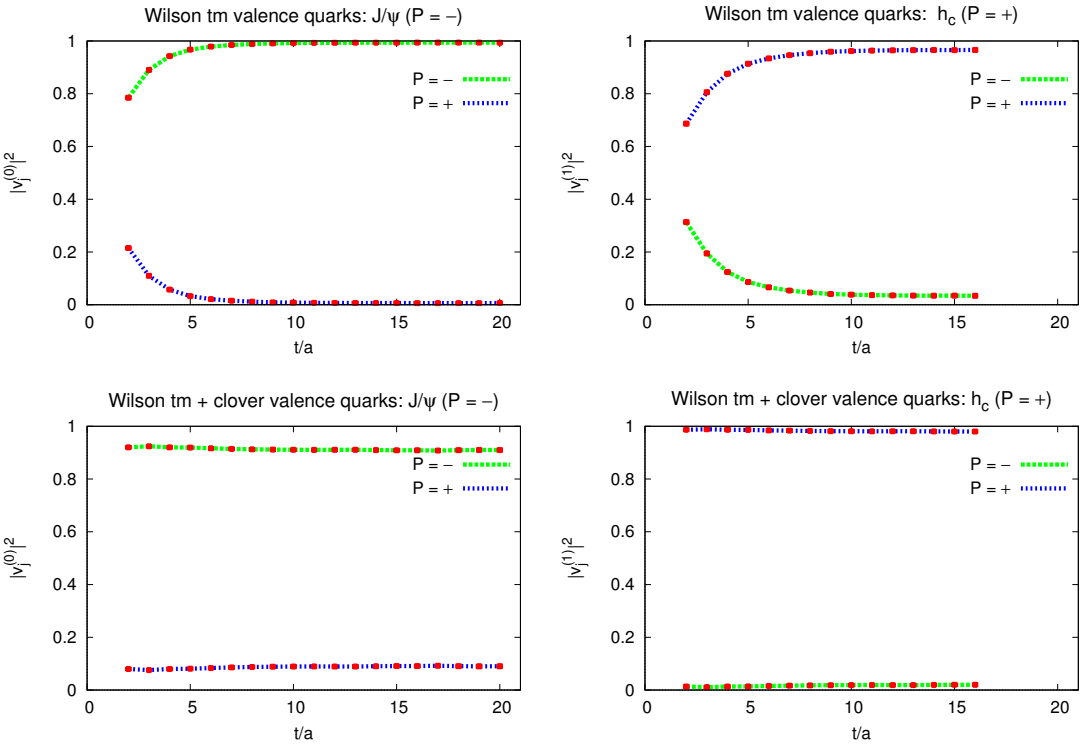

Figure 13: Squared absolute eigenvector components for the J/ψ and h_c meson for Wilson twisted mass valence quarks, with and without clover term. Column line graphs show the behavior for states of equal parity.

In case of the vector mesons J/ψ and h_c the appearance of the squared absolute eigenvector components in the Wilson twisted mass setup is noticeably affected by the addition of the clover term. For Wilson twisted mass valence quarks an overlap to the opposite parity partner for small temporal separations can be observed. This effect decreases with an increasing temporal separation and flattens down to a small contribution of parity mixing effects, even vanishing effects for the pseudo scalar state.
Strangely it appears that the addition of the clover term has even a negative effect on the parity mixing contributions of the ground state mass. There no overlap dependence for small temporal separations is observed anymore, but the mixing contributions remain constant at $< 10\%$.

The pseudo vector state on the other hand seems to improve around the same order as previously the $P = -$ state for the D meson did after addition of the clover term.

3.4 Mass splitting

As already stated, earlier in this work, besides the explicit breaking of parity symmetry the Wilson twisted mass formulation of lattice QCD also suffers from an explicit breaking of isospin symmetry. Effects of this broken symmetry are for example a splitting in masses between charged and connected neutral pions. This effect is expected to be the largest in the splitting of the lightest charged and uncharged pseudo scalar meson.

3.4.1 Light pseudo scalar sector

In this section a rather qualititative presentation of isospin breaking effects for the Wilson twisted mass lattice discretization is given in the light pseudo scalar sector.

In figure 14 the effective masses of the charged and connected neutral pseudo scalar meson with Wilson twisted mass and Wilson twisted mass + clover valence quarks is given. The operators used are $O_j \in \{\bar{\chi}^{(u)}\gamma_5\chi^{(d)}, \bar{\chi}^{(u)}\chi^{(u)} + \bar{\chi}^{(d)}\chi^{(d)}\}$ generating the respective quantum numbers of $J^P = 0^-$ and $J^P = 0^-$ when applied to the vacuum.

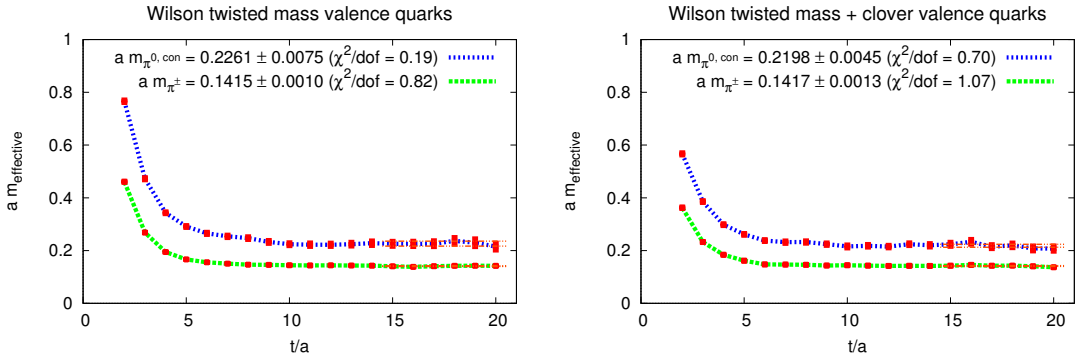

Figure 14: Pion mass splitting as consequence of broken isospin symmetry for Wilson twisted mass valence quarks without and with clover term. (Each plot contains two individual mass plateaus, not to be mistaken with the solution for the generalized eigenvalue problem).

Expressing the pion mass splitting as numerical value

$$\Delta(m_\pi)^2 \equiv \left| m^2_{\pi^\pm} - m^2_{\pi^{0,\mathrm{con.}}} \right|, \tag{3.10}$$

where "con." denotes the fact, that disconnected diagrams are omitted. Those are technically difficult to compute and are vanishing once the continuum is reached. The pion mass splitting can be precisely determined for both action setups to

$$a^2\Delta(m_\pi^{\mathrm{tm}})^2 = 0.0311(37), \quad a^2\Delta(m_\pi^{\mathrm{tm+clover}})^2 = 0.0282(23). \tag{3.11}$$

Within errors the coefficient of the light pseudo scalar mass splitting is thus unchanged to the original unitary setup.
This observation is in contrast with a similar quenched investigation [5], where a beneficial effect in reducing cutoff effects related to isospin breaking is observed.

The obtained results for the expected reduction of isospin breaking effects are at this point of negligible magnitude. This implies a not present reduction of the $\mathcal{O}(a^2)$ lattice discretization effects after the application of the clover term to the Wilson twisted mass action.
Regarding the rather inconclusive results of the study so far a further, more critical analysis on the correct application of the clover term, or more precisely on the correct choice of the Sheikoleslami Wohlert coefficient c_{sw} may be desirable. The tuning process (cf. section 3.2) is however a rather time consuming task, requiring a precise determination of input parameters to ensure validity of the computed observables.
With the purpose of a quick review on the impact of the clover term, requiring only minimal tuning efforts, an analysis of the pion mass splitting in a range of Sheikoleslami Wohlert coefficients c_{sw} is shown in figure 15.
Demanding only a PCAC mass of $\mathcal{O}(10^{-3})$ the previously precise determined value (3.8), with a criterion of $|m_{\text{PCAC}}|/\mu \leq 0.1$, is obviously exceeded. Additionally a further tuning of the light quark mass was omitted, keeping $a\mu = 0.004$ constant in this section. Since both $\pi^{\pm}$ and $\pi^{0,\text{con}}$ are computed with the same light quark mass it is expected, that the difference is rather independent of μ.

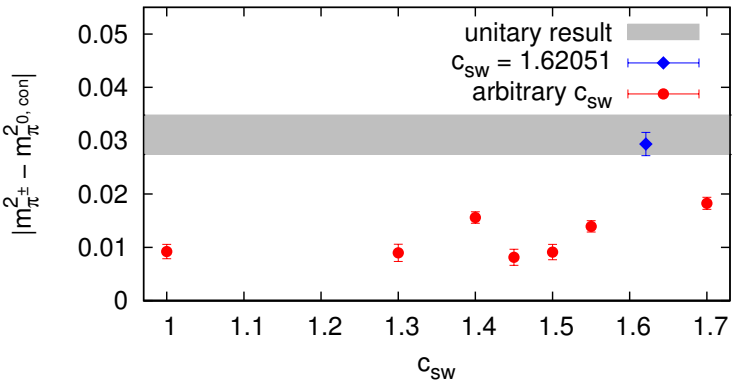

Figure 15: Pion mass splitting of Wilson twisted mass + clover valence quarks for several c_{sw} coefficients with a constant light quark mass of $a\mu = 0.0040$.

What is observed is, that for none of the arbitrary c_{sw} coefficients a pion mass splitting $\Delta(m_\pi)^2$ as large as for the unitary setup or for $c_{\text{sw}} = 1.62051$ was found, i.e. every arbitrary c_{sw} coefficient had a significant reduction of the isospin breaking as a consequence.

3.4.2 Heavy sector

Extending the observation of the charged/neutral mass splitting to the heavy quark sector, further observations were made.

The operators used are $O_j \in \{\bar{\chi}^{(c^+)}\gamma_k\gamma_5\chi^{(c^-)}, \bar{\chi}^{(c^+)}\gamma_k\chi^{(c^-)}\}$ for the neutral states and $O_j \in \{\ \bar{\chi}^{(c^-)}\gamma_k\chi^{(c^-)}, \bar{\chi}^{(c^-)}\gamma_k\gamma_5\chi^{(c^-)}\}$ for the charged states.

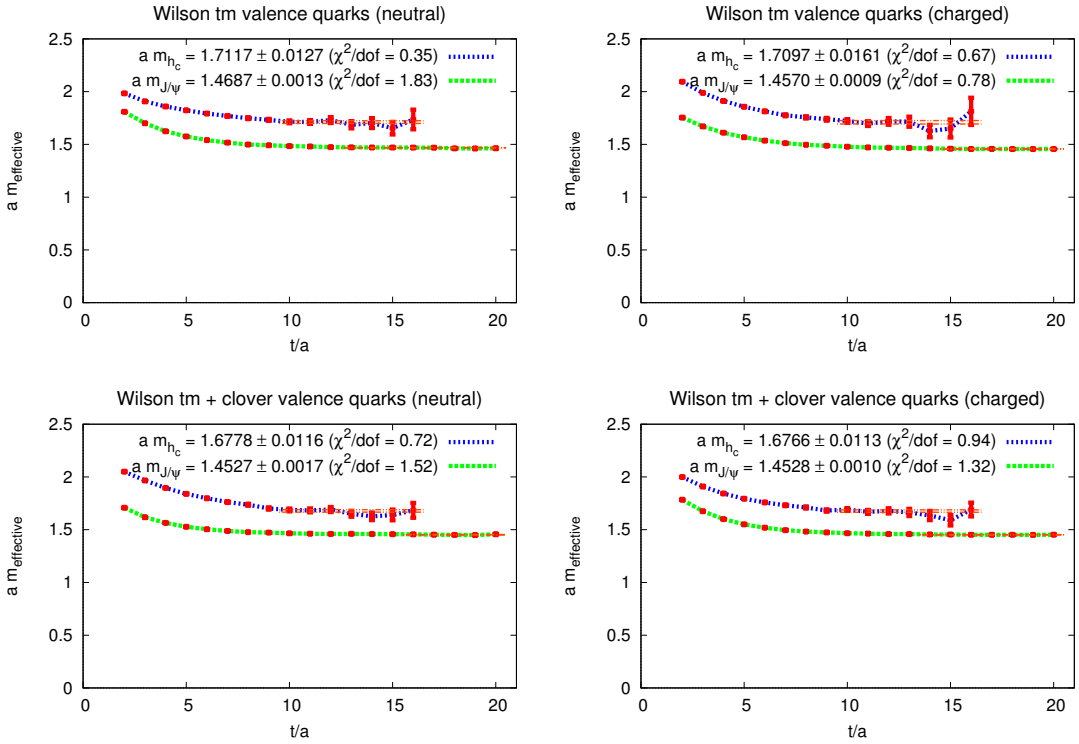

Figure 16: Effective masses of the charged and neutral J/ψ and h_c meson, obtained for Wilson twisted mass valence quarks, as a function of temporal separation t/a.

Considering that the isospin breaking effects are small in the heavy quark sector, compared to the light quark sector, a great reduction of isospin breaking effects for the pseudo vector state J/ψ could be found. The masses of the charged and neutral J/ψ are nearly identical for the coefficient $c_{\text{sw}} = 1.62051$, where for the excited state a similar, but more cautious statement can be made, due to the large noise in both setups.
Similar effects for the D meson were not obtained.

4 Summary, Conclusion and Outlook

In this work, results for mixed action setups of lattice QCD with $N_f = 2+1+1$ maximal twisted Wilson twisted mass sea quarks at a fixed value of the lattice spacing were presented. With $a \approx 0.086$ fm the corresponding pseudo scalar mass was of about 320 MeV. The main purpose was to find a mixed action setup more suited for mass spectroscopy, than the unitary setup with Wilson twisted mass fermions. This was performed with a focus on simple quantities from the light scalar and heavy scalar quark sector. With a single lattice spacing the expected reduction of discretization effects was studied with the use of observables, that suffer from symmetry breaking effects.

4.1 Summary

In order to investigate mixed action setups the tuning, where sea and valence quarks are matched with suitable conditions, is of central importance. Only by doing so the continuum limit of observables is identical for all setups, making a comparison of the discretization errors possible. Employing Wilson twisted mass quarks in the sea, the mixed actions were generated with Wilson twisted mass quarks, standard Wilson quarks and an extension of both these actions by addition of the clover term.

With a rather simple concept of the clover action S_{clover} the main difficulty is the determination of the c_{sw} coefficient. For the computations in this work a value computed by a perturbative expansion [29] was chosen, suiting to the used ensemble.

The tuning process of both Wilson valence quark actions was then quite similar. With a fixed $a\mu = 0$ only one parameter remained for the adjustment. Where the Wilson valence action was in comparison quickly tuned, due to an accelerated inversion of the Dirac operator, a noticeable increase in the statistical noise of the pseudo scalar mass raised first suspicions concerning this action setup. The addition of the clover term to the Wilson valence caused a further increase in the inversion time and resulted in the inability of a clear computation of the pseudo scalar mass am_{PS}. This behavior is probably caused due to a further decrease in the pseudo scalar mass, after mass-like contributions coming from the clover term where added, effectively forcing computations close to the critical value and so below the unitary pseudo scalar mass.

Assuming an identical c_{sw} coefficient for the Wilson twisted mass valence action, the tuning process for this setup was more complicated due to the existence of two input parameters. At first the critical value for the bare untwisted quark mass had to be found, restoring theory at maximal twist and ensuring a reduction to $\mathcal{O}(a^2)$ lattice discretization effects. After restoring maximal twist a slight shift in pseudo scalar masses could be observed, rising necessity of an additional tuning in the twisted mass parameter to restore unitary results. For tuning of the quark mass μ the linear behavior of am_{PS}^2 in $a\mu$ lead to quick results.

Completing the tuning process comparable computations of observables were available, for all action setups. In section 3.3 effective mass computations for the $D(J^P = 0^-)$, $D_0^*(J^P = 0^+)$, $J/\psi(J^P = 1^-)$ and $h_c(J^P = 1^+)$ as function of the temporal separation t/a, as well as their composition in terms of squared absolute eigenvector components were presented.
Results obtained for the masses of the D mesons are in all four mixed action setups in agreement within errors. Application of Wilson valence quarks, with parity as exact symmetry of this lattice formulation, was expected to produce drastically improved results for the mass plateaus of scalar states, in comparison to Wilson twisted mass at maximal twist. Instead of a mass plateau comparable to the low lying pseudo scalar state, the statistical noise resulted in a plateau similar to the unitary setup. Addition of the clover term to the unimproved action, even worsened the results. For Wilson twisted mass quark however the clover term effectively left the unitary results unchanged, but increased the temporal separation of the mass plateau. Analyzing the squared absolute eigenvector components, an indication for a reduction of parity mixing effects was observed.
Computations for the vector meson J/ψ and its parity partner h_c, showed comparable results. Both Wilson twisted mass action setups, as well as the clover improved Wilson action provided comparable masses for the J/ψ. The scalar mass for Wilson twisted mass quarks was unchanged by the addition of the clover action. Unimproved Wilson quarks showed a noticeable difference in the pseudo scalar mass value, which could come from remaining $\mathcal{O}(a)$ effects.
Comparison of the squared eigenvector components between Wilson twisted mass and Wilson twisted mass + clover valence quarks indicated a corruption of the parity mixing for the pseudo scalar state. This was a quite surprising effect, which is not yet completely understood and requires further analysis. Mixing contributions for the scalar state however implied a reduction in the parity mixing of the same order as for the D meson.

In the last section, a brief investigation of isospin breaking effects in the light scalar sector, after application of the clover term to the Wilson twisted mass action, was intended. Similar to parity breaking effects the addition of the clover term was expected to reduce isospin breaking effects, as $\mathcal{O}(a^2)$ lattice discretization effects, as well. What was observed is that no reduction is present for the coefficient of $c_{\mathsf{sw}} = 1.62051$. Instead it was observed, that every other arbitrary c_{sw} coefficient does in fact reduce the pion mass splitting.
In the heavy quark sector great reductions in the mass splitting for the pseudo scalar J/ψ were observed, though these results were not present for the D meson.

4.2 Conclusion & Outlook

In this work three different mixed action setups were studied and compared to a unitary setup with twisted mass fermions. Regarding an improvement for mass spectroscopy the following can be stated:

- Wilson fermions in the valence action suffer from $\mathcal{O}(a)$ lattice discretization effects and are so not favored for computations.
- Application of the clover term to the Wilson valence action is supposed to improve the theory, but the encountered inability to compute the pion mass makes this setup extremely questionable.
- Results obtained from twisted mass valence fermions with clover term are still inconclusive. No crucial change after the application of the clover term was observed, despite the fact of an expensive tuning.

An interesting aspect, which has not been investigated here is the use of different lattice spacings. Without the need of observables, that imply a reduction of discretization effects, an expected accelerated continuum convergence could been studied there.

So far the unitary approach with Wilson twisted mass valence quarks appears to be the most suitable setup for mass spectroscopy, compared to the others.
However, an increased impact in the reduction of isospin breaking effects were observed for different c_{sw}. Although a reduction of isospin breaking effects does not necessarily imply a present reduction in parity effects, a minimum in $\Delta(m_\pi)^2$, or reducing it to zero, would let the corresponding c_{sw} become an attractive candidate for further investigations.

Acknowledgements

In the following the author would like to thank several people for their help and support on writing this Master thesis:

Marc Wagner, as supervisor of this work, at first for giving me the possibility to write my thesis in this field. He had literally always an open door and the discussions where not only helpful, but motivating for the further work.

David Palao for his persistent interest and attentive guidance of this works progress. His experience in this field induced me to work more rigorous and saved me from possible dead ends.

Martin Kalinowski for the kind introduction into the topic, explanation of numerous numerical applications and the continuous exchange throughout the last year.

Georg Bergner and Wolfgang Unger, my office colleagues, for the nice atmosphere and being always on hand with help and advice.

Andrea Shindler, Urs Wenger and Gregorio Herdoiza for very helpful discussions.

This work was supported in part by the Helmholtz International Center for FAIR with the framework of the LOEWE program launched by the State of Hesse.

References

[1] K. G. Wilson, Phys. Rev. D **10** (1974) 2445.

[2] R. Frezzotti *et al.* [Alpha Collaboration], JHEP **0108** (2001) 058 [hep-lat/0101001].

[3] R. Frezzotti and G. C. Rossi, JHEP **0408** (2004) 007 [hep-lat/0306014].

[4] K. Jansen *et al.* [XLF Collaboration], Phys. Lett. B **624** (2005) 334 [hep-lat/0507032].

[5] D. Becirevic, P. Boucaud, V. Lubicz, G. Martinelli, F. Mescia, S. Simula and C. Tarantino, Phys. Rev. D **74** (2006) 034501 [hep-lat/0605006].

[6] P. Boucaud *et al.* [ETM Collaboration], Phys. Lett. B **650** (2007) 304 [hep-lat/0701012].

[7] B. Kostrzewa, "Preliminary results from maximally twisted mass lattice QCD at the physical point", unpublished.

[8] C. Alexandrou, J. O. Daldrop, M. Dalla Brida, M. Gravina, L. Scorzato, C. Urbach and M. Wagner, JHEP **1304** (2013) 137 [arXiv:1212.1418].

[9] M. Kalinowski and M. Wagner, PoS ConfinementX (2012) 303 [arXiv:1212.0403 [hep-lat]].

[10] M. Kalinowski and M. Wagner, Acta Physica Polonica B Proceedings Supplement vol. **6** (2013) page 991 [arXiv:1304.7974 [hep-lat]].

[11] J. Berlin, D. Palao and M. Wagner, arXiv:1308.4916 [hep-lat].

[12] A. Shindler, Phys. Rept. **461** (2008) 37 [arXiv:0707.4093 [hep-lat]].

[13] S. Sint, hep-lat/0702008 [HEP-LAT].

[14] C. Gattringer and C. B. Lang, Lect. Notes Phys. **788**, (2010).

[15] H. J. Rothe, World Scientific Lect. Notes Phys. - Vol. **74** (2005).

[16] U. J. Wiese, "An introduction to lattice field theory" (2009).

[17] I. Montvay and G. Münster, Cambridge University Press (1994).

[18] T. DeGrand and C. E. Detar, World Scientifc Publishing Co. Pte. Ltd. (2006).

[19] R. Frezzotti and G. C. Rossi, Nucl. Phys. Proc. Suppl. **128** (2004) 193 [hep-lat/0311008].

[20] R. Baron *et al.* [European Twisted Mass Collaboration], Comput. Phys. Commun. **182** (2011) 299 [arXiv:1005.2042 [hep-lat]].

[21] Y. Iwasaki, Nucl. Phys. B **258**, 141 (1985).

[22] B. Sheikholeslami and R. Wohlert, Nucl. Phys. B **259** (1985) 572.

[23] C. Wiese, Master thesis (2012).

[24] P. Boucaud *et al.* [ETM Collaboration], Comput. Phys. Commun. **179** (2008) 695 [arXiv:0803.0224 [hep-lat]].

[25] K. Jansen and C. Urbach, Comput. Phys. Commun. **180** (2009) 2717 [arXiv:0905.3331 [hep-lat]].

[26] C. Urbach, K. Jansen, A. Shindler and U. Wenger, Comput. Phys. Commun. **174** (2006) 87 [arXiv:hep-lat/0506011].

[27] B. Blossier, M. Della Morte, G. von Hippel, T. Mendes and R. Sommer, JHEP **0904** (2009) 094 [arXiv:0902.1265 [hep-lat]].

[28] R. Baron, P. Boucaud, J. Carbonell, A. Deuzeman, V. Drach, F. Farchioni, V. Gimenez and G. Herdoiza *et al.*, JHEP **1006** (2010) 111 [arXiv:1004.5284 [hep-lat]].

[29] S. Aoki, R. Frezzotti and P. Weisz, Nucl. Phys. Proc. Suppl. **73** (1999) 915 [hep-lat/9809179].